Cellular models for fundamental and applied biomedical research

Liu, J.

Chapter 6

Allosteric Modulation of $K_v11.1$ (hERG) Channels Protects against Drug-Induced Ventricular Arrhythmias

Zhiyi Yu*; Jia Liu*; Jacobus P.D. van Veldhoven; Adriaan P. IJzerman; Martin J. Schalij; Daniël A. Pijnappels; Laura H. Heitman#; Antoine A. F. de Vries#

*,#Equal contribution

Adapted from: Circ Arrhythm Electrophysiol. 2016;9:e003439.

Abstract

Background-Ventricular arrhythmias due to unintentional blockade of the $K_v11.1$ (hERG) channel are a major safety concern in drug development. In past years, several highly prescribed drugs have been withdrawn for their ability to cause such proarrhythmia. Here, we investigated whether the proarrhythmic risk of existing drugs could be reduced by $K_v11.1$ allosteric modulators.

Methods and Results-Using [^{3}H]dofetilide binding assays with membranes of human $K_v11.1$-expressing HEK293 cells, two existing compounds (VU0405601 and ML-T531) and a newly synthesized compound (LUF7244) were found to be negative allosteric modulators of dofetilide binding to the $K_v11.1$ channel with LUF7244 showing the strongest effect at 10μM. The $K_v11.1$ affinities of typical blockers (*i.e.*, dofetilide, astemizole, sertindole and cisapride) were significantly decreased by LUF7244. Treatment of confluent neonatal rat ventricular myocyte (NRVM) monolayers with astemizole or sertindole caused heterogeneous prolongation of action potential (AP) duration and a high incidence of early afterdepolarizations upon 1-Hz electrical point stimulation, occasionally leading to unstable, self-terminating tachyarrhythmias. Pretreatment of NRVMs with LUF7244 prevented these proarrhythmic effects. NRVM monolayers treated with LUF7244 alone displayed electrophysiological properties indistinguishable from those of untreated NRVM cultures. Prolonged exposure of NRVMs to LUF7244 or LUF7244 plus astemizole did not affect their viability, excitability and contractility as assessed by molecular, immunological and electrophysiological assays.

Conclusion-Allosteric modulation of the $K_v11.1$ channel efficiently suppresses drug-induced ventricular arrhythmias in-vitro by preventing potentially arrhythmogenic changes in AP characteristics, raising the possibility to resume the clinical use of unintended $K_v11.1$ blockers via pharmacological combination therapy.

Introduction

Drug-induced ventricular arrhythmias (DiVAs) are a frequently encountered clinical problem, which has resulted in restricted use or market withdrawal of existing cardiac and non-cardiac drugs and still represents a major obstacle for the development of new drugs.[1] Inhibition of the rapid component of the delayed rectifier K^+ current (I_{Kr}) has been identified as the major culprit in the development of DiVAs. The consequential slowing of cardiac repolarization, manifested in the surface electrocardiogram as a prolongation of the QT interval, increases the likelihood of early afterdepolarizations (EADs), which may give rise to ectopic beats. Drug-induced I_{Kr} blockade also increases spatial dispersion of repolarization and refractoriness thereby further increasing proarrhythmic risk.[2] Together these electrophysiological alterations promote the development of a special type of polymorphic ventricular arrhythmias known as "Torsades de Pointes" (TdPs), which mostly resolve spontaneously but occasionally degenerate into fatal ventricular fibrillation.[3] The K_v11.1 protein, which is encoded by the KCNH2 gene (also known as ether-à-go-go–related gene 1 [ERG or ERG1]), represents the pore-forming α-subunit of the I_{Kr} channel.[4] Several structural features of K_v11.1 render the central cavity of the I_{Kr} channel particularly susceptible to blockade by a heterogeneous collection of chemical compounds including various non-cardiac drugs (e.g., astemizole, sertindole and cisapride).

An obvious strategy to reduce the proarrhythmic risk of drugs with unintended I_{Kr}-blocking effects is by lowering their K_v11.1 affinities via chemical modifications. Alternatively, supplementary drugs that decrease the proarrhythmic risk of inadvertent K_v11.1 blockers can be developed potentially allowing (i) reintroduction of medicines previously recalled from the market because of their K_v11.1-related cardiotoxicity and (ii) admission of new drugs with fortuitous I_{Kr}-blocking activity. Paradoxically, screening of drugs for possible I_{Kr}-blocking side effects has resulted in the serendipitous discovery of various K_v11.1 activators.[5] Besides their potential usefulness in treating inherited long QT syndrome (LQTS), these K_v11.1 activators may also be used to counteract K_v11.1 blockade-associated DiVAs. Indeed, Kang *et al*. showed that the action potential (AP) duration (APD)-prolonging effect of the I_{Kr}-blocking, class III antiarrhythmic drug dofetilide could be counterbalanced by the first identified synthetic K_v11.1 activator designated RPR260243.[6] However, due to their APD-shortening effect, K_v11.1 activators may induce short QT syndrome.[5] Recently, Potet *et al*. described a compound designated VU0405601 that upon pretreatment significantly reduced the APD-prolonging effect of dofetilide in Langendorff-perfused rabbit hearts and dose-dependently mitigated the K_v11.1-blocking effects of seven different drugs in HEK293 cells stably overexpressing the human KCNH2 gene (HEK293K_v11.1 cells).[7] VU0405601 exerted its effects on the K_v11.1 channel in whole-cell voltage-clamp experiments using HEK293K_v11.1 cells only when applied extracellularly. This suggests that VU0405601 binds to the extracellular domain of the K_v11.1 channel rather than to its central cavity leading us to hypothesize that VU0405601 counteracts the APD-prolonging effect of K_v11.1 blockers by an allosteric mechanism.

Allosteric modulators bind their targets at a site topologically different from that of the endogenous ligand. From this so-called allosteric site they generally display higher selectivity across receptor subtypes and thus provide a safer pharmacological profile than ligands binding to the orthosteric site.[8] Notably, since the $K_v11.1$ channel does not have an endogenous ligand, the authors refer to the site where typical blockers (*i.e.*, dofetilide and astemizole) bind as the orthosteric site. Whereas allosteric modulators targeting ligand-gated ion channels and G protein-coupled receptors have been well established as research tools and therapeutic agents,[8-10] little progress has been made in the discovery and clinical development of such compounds for voltage-gated ion channels.

In this study, in-vitro radioligand binding assays were used to investigate whether two previously reported compounds (*i.e.*, VU0405601[7] and ML-T531[11]) and a new compound designated LUF7244 could allosterically modulate binding of the potent $K_v11.1$ blocker dofetilide to the channel's central cavity.[12,13] Radioligand binding assays were also employed to study LUF7244's influence on the interaction between (i) the $K_v11.1$ channel and three different blockbuster drugs (*i.e.*, astemizole, sertindole and cisapride) that have been withdrawn from the market due to their $K_v11.1$-related cardiotoxicity[14] and (ii) astemizole and its intended target, the human histamine H_1 receptor (hH_1R, see **Data Supplement**). The radioligand binding assays were complemented with optical voltage mapping experiments in confluent monolayers of neonatal rat ventricular myocytes (NRVMs). These experiments were performed in the absence and presence of LUF7244 and/or any of the three blockbuster drugs. Electrophysiological parameters analyzed included conduction velocity (CV), APD at 40 and 90% repolarization (APD_{40} and APD_{90}, respectively), APD dispersion and EAD incidence. In addition, the effects of LUF7244 alone and together with astemizole on the viability, excitability and contractility of NRVMs were investigated (see **Data Supplement**). The results of this study indicate that negative allosteric modulation of the $K_v11.1$ channel may provide a safe and effective means to prevent the proarrhythmic effects of I_{Kr} blockers that bind to the channel's central cavity.

Materials and Methods

Radioligand Binding Studies

Radioligand displacement assays and kinetic dissociation assays were performed on membranes of HEK293K_v11.1 cells using [^{3}H]dofetilide as radioligand essentially as described before.[15]

Isolation and Culture of NRVMs

NRVMs were isolated from the hearts of neonatal rats and cultured as previously detailed.[16] The use of these animals was approved by the Animal Experiments Committee of Leiden University Medical Center and conformed to the Guide for the Care and Use of Laboratory Animals as stated by the US National Institutes of Health.

Immunocytochemical Analyses

NRVMs were plated on fibronectin-coated, 15-mm diameter round glass coverslips at a density of 4×10^4 cells. At day 9 of culture, the cells were washed with ice-cold phosphate-buffered saline (PBS), fixed in buffered 4% formaldehyde and permeabilized with 0.1% Triton X-100 in PBS. Next, the cells were double-immunostained for Kv11.1 and α-actinin. Incubation with primary antibodies (diluted 1:200 in PBS-0.1% normal donkey serum) and corresponding donkey Alexa Fluor 488/568-conjugated secondary antibodies (1:400 dilution) lasted for 2 hours. To visualize their nuclei, the cells were incubated with 10µg/mL Hoechst 33342 in PBS. After each processing step, the cells were washed with PBS. Coverslips were mounted in VECTASHIELD mounting medium. Photomicrographs were obtained using a Nikon Eclipse 80i digital color camera-equipped fluorescence microscope.

Reverse Transcription-Quantitative Polymerase Chain Reaction Analyses

Total RNA extracted from NRVMs and from neonatal rat cardiac fibroblasts (NRCFs; maintained in NRVM medium) using the QIAGEN RNeasy Mini kit was reverse transcribed with the Bio-Rad iScript cDNA synthesis kit and the resulting cDNA was amplified by PCR using the Bioline SensiFAST SYBR No-ROX kit. PCR amplifications of rat Kcnh2- and rat 18S rRNA (Rn18s)-specific cDNA (for primer sequences, see **Data Supplement**) were carried out in a CFX96 Touch Real-Time PCR detection system (Bio-Rad) using a 2-step cycling protocol (20-40 cycles of 95°C 10 sec, 60°C 30 sec) after a 5-minute incubation at 95°C. Quantitative analyses were based on the $2^{-\Delta\Delta CT}$ method using CFX Manager software (Bio-Rad).

Optical Mapping Experiments

Optical mapping experiments were done in confluent monolayers of NRVMs using the potentiometric dye di-4-ANEPPS as voltage indicator following previously described methods.[17] To validate the experimental model, cells were incubated for 20 minutes in culture medium containing 0, 10, 30, 100 or 300nM of the hH_1R antagonist and unintended K_v11.1 blocker astemizole and dimethylsulfoxide (DMSO) at a final concentration of 0.03%. In a subsequent experiment, NRVM cultures were first exposed for 30 minutes to 10µM LUF7244 or its solvent (*i.e.*, culture medium containing 0.1% DMSO). Next, astemizole (final concentration of 100nM) or vehicle

was added to the culture medium raising the DMSO concentration to 0.13%. Following an incubation period of 30 minutes at 37°C, optical recordings were started in the continued presence of the appropriate vehicle/drug combinations.

Data Analysis

Radioligand binding assay data were analyzed with GraphPad Prism 5.0 (GraphPad Software, San Diego, CA). Half maximal inhibitory concentrations (*i.e.*, IC_{50} values), apparent inhibitory binding constants (K_i values), dissociation rate constants (k_{off}) and half maximal effective concentrations (*i.e.*, EC_{50} values) were calculated as previously described.[18] Values obtained from the radioligand binding assays are from three different experiments each consisting of two independent samples. Data are expressed as mean±standard error of the mean (SEM) for the radioligand binding assays or as mean±standard deviation (SD) for the optical voltage mapping experiments.

See the **Data Supplement** for more details about the materials and experimental procedures.

Results

Characterization of Allosteric Modulators of [^{3}H]Dofetilide Binding to the K_v11.1 Channel

The interaction of two previously reported ligands VU405601 and ML-T531 as well as the newly designed and synthesized compound LUF7244 (**Figure 1A**) with the human K_v11.1 channel was studied in different [^{3}H]dofetilide binding assays. As shown in **Figure 1B** and **Table I** in the **Data Supplement**, all three compounds reduced [^{3}H]dofetilide binding to the K_v11.1 channel with relatively low affinities, *i.e.*, with IC_{50} values of 7.8±0.4μM, 12±1μM and 3.9±0.7μM for VU0405601, ML-T531 and LUF7244, respectively. Moreover, all displacement curves demonstrated Hill coefficients different from unity (*i.e.*, -1.1±0.03 for ML-T531, -1.2±0.01 for VU0405601 and -1.3±0.1 for LUF7244), implying that VU0405601, ML-T531 and LUF7244 might not competitively displace [^{3}H]dofetilide from the K_v11.1 channel but may bind elsewhere to the channel protein to allosterically modulate radioligand binding.

Subsequently, single-point dissociation assays were performed to screen for allosteric effects of these compounds on the binding of [^{3}H]dofetilide to the K_v11.1 channel. At a concentration of 10μM, VU0405601, ML-T531 and LUF7244 significantly increased the dissociation of [^{3}H]dofetilide from the K_v11.1 channel, indicating that these compounds are negative allosteric modulators of dofetilide binding to the channel (**Figure 1C** and **Table I** in the **Data Supplement)**. LUF7244 appeared to be the most potent negative allosteric modulator with 44±2% dofetilide binding left compared to control conditions, while 10μM VU0405601 and ML-T531 reduced dofetilide binding to 63±3% and 77±3%, respectively.

The allosteric effects of VU0405601, ML-T531 and LUF7244 on the K_v11.1 channel were further investigated in traditional radioligand dissociation experiments to determine whether co-administration of these compounds with an excess unlabeled dofetilide would change the dissociation rate of [^{3}H]dofetilide from the K_v11.1 channel. To obtain larger effects, the three compounds were tested at a concentration

of 50μM instead of 10μM as used in the single-point dissociation assays. As shown in **Figure 1D** and **Table I** in the **Data Supplement**, all compounds significantly accelerated the dissociation of dofetilide, in line with the results from the single-point dissociation experiments. The off-rate of [^{3}H]dofetilide was allosterically increased 2.0-fold (from 0.21±0.02 to 0.42±0.04min^{-1}) with 50μM VU0405601. The k_{off} value of [^{3}H]dofetilide rose to 0.33±0.02min^{-1} in the presence of 50μM LUF7244, which was comparable to the effect of ML-T531 ($k_{off,dofetilide}$=0.30±0.03min^{-1}).

Effects of LUF7244 on the Binding of Typical K_v11.1 Blockers to the Channel

Since LUF7244 was the most potent amongst the three allosteric modulators at the lower test concentration of 10μM and may therefore have the best safety profile, its potency to increase the dissociation of [^{3}H]dofetilide from the K_v11.1 channel was investigated. From the corresponding concentration-effect curve (**Figure 2A**), the modulatory potency (*i.e.*, the EC_{50}) of LUF7244 was calculated to be 4.6±0.8μM. Notably, LUF7244 could not completely abrogate [^{3}H]dofetilide binding by accelerating its dissociation from the K_v11.1 channel.

To investigate the effects of LUF7244 on the binding affinities of other compounds besides dofetilide to the K_v11.1 channel, three additional K_v11.1 blockers (*i.e.*, astemizole, sertindole and cisapride) from distinct therapeutic classes were selected (**Figure 2B**). As shown in **Figure 2C-D**, the [^{3}H]dofetilide displacement curves of all four drugs were shifted rightwards in the presence of 10μM LUF7244, implicating that their K_v11.1 affinities were diminished by this negative allosteric modulator. The K_i values of dofetilide, astemizole, sertindole and cisapride in the absence or presence of 10μM LUF7244 are listed in **Table II** of the **Data Supplement**. LUF7244 most strongly modulated cisapride binding to the K_v11.1 channel, increasing its K_i value by 4.0-fold from 21±1 to 85±6nM. Similarly, the K_v11.1 affinities of astemizole, dofetilide and sertindole were reduced by 3.8-, 3.2- and 2.2-fold in the presence of LUF7244. Thus, the negative allosteric effect of LUF7244 on the K_v11.1 channel significantly lowered the channel's affinities for several chemically and therapeutically distinct K_v11.1 blockers.

Analysis of K_v11.1 Protein Expression in NRVMs

Next, the electrophysiological consequences of allosteric modulation of the binding of typical K_v11.1 blockers to the channel by LUF7244 (see **Figure 3A** for experimental setup) were examined in confluent monolayers of NRVMs (**Figure 3B**) as relevant in-vitro model for studying cardiac arrhythmias.[19] Double immunostaining for K_v11.1 and sarcomeric α-actinin showed that all cardiomyocytes in the NRVM cultures expressed the K_v11.1 protein (**Figure 3C**). The K_v11.1 signal had a punctate or linear appearance and was concentrated around nuclei and along the sarcolemma (**Figure 3C**). No significant K_v11.1 protein expression was observed in the low percentage of α-actinin$^-$ cells (mainly NRCFs) present in the NRVM cultures. Consistently, comparison of *Kcnh2* transcript levels between NRVMs and NRCFs by reverse transcription-polymerase chain reaction (RT-PCR) analysis demonstrated ± 40-fold higher Kcnh2 mRNA expression in NRVMs than in NRCFs (**Figure 3D**).

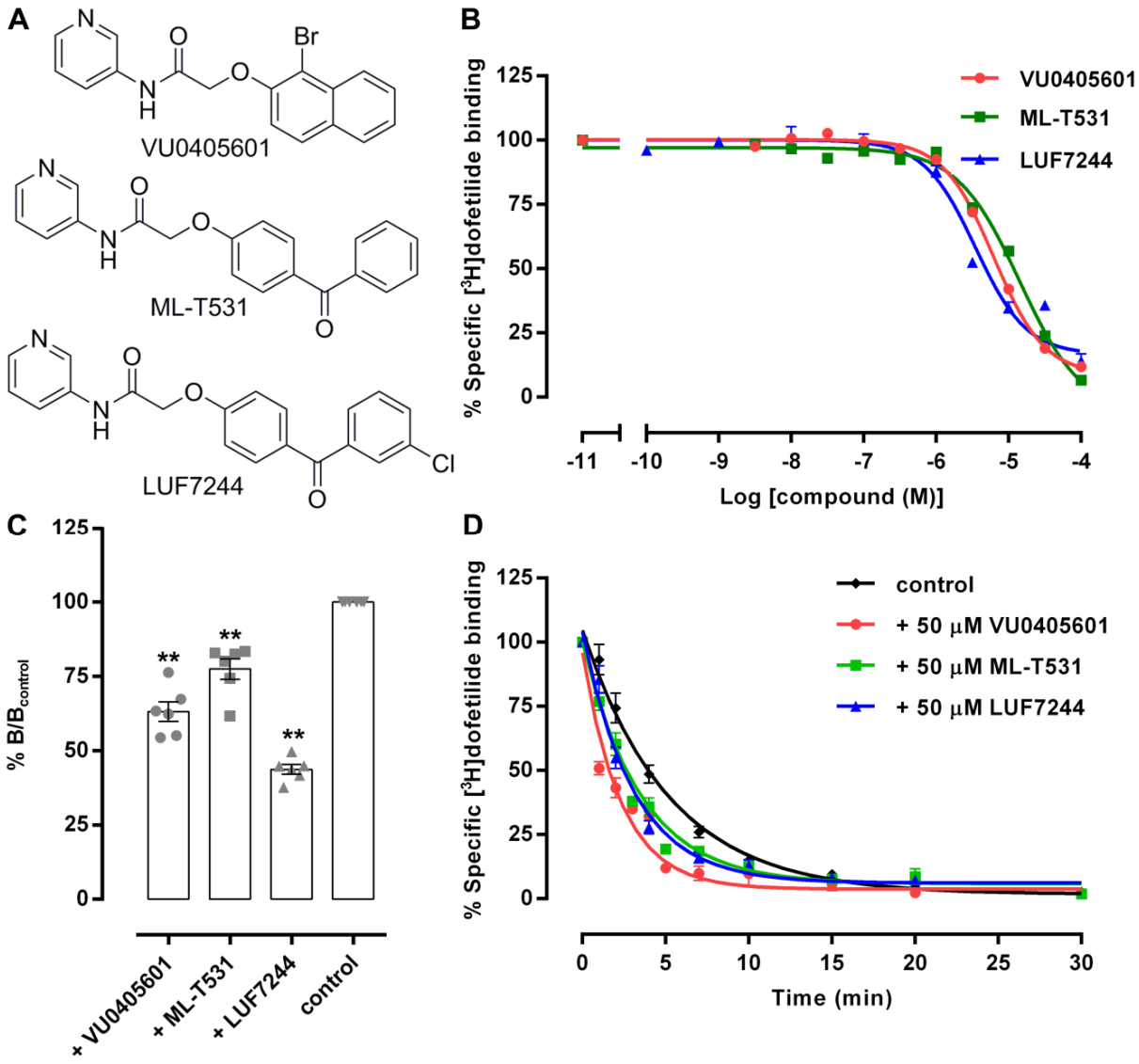

Figure 1. Characterization of allosteric modulators of dofetilide binding to the K_v11.1 channel in a [^{3}H]dofetilide binding assay performed with membranes of HEK293K_v11.1 cells. A: Chemical structures of VU0405601, ML-T531 and LUF7244. B: Displacement curves of VU0405601, ML-T531 and LUF7244. C: Percentage specific binding of [^{3}H]dofetilide to the K_v11.1 channel after 6 minutes of dissociation induced by 10µM dofetilide in the absence (control) or presence of 10µM of VU0405601, ML-T531 or LUF7244. The specific binding of [^{3}H]dofetilide in the absence of the test compounds was set as $B_{control}$, while the specific binding in their presence was set as B. $^{**}P<0.01$. D: Time-dependent dissociation of [^{3}H]dofetilide induced by 10µM dofetilide in the absence (control) or presence of 50µM VU0405601, ML-T531 or LUF7244.

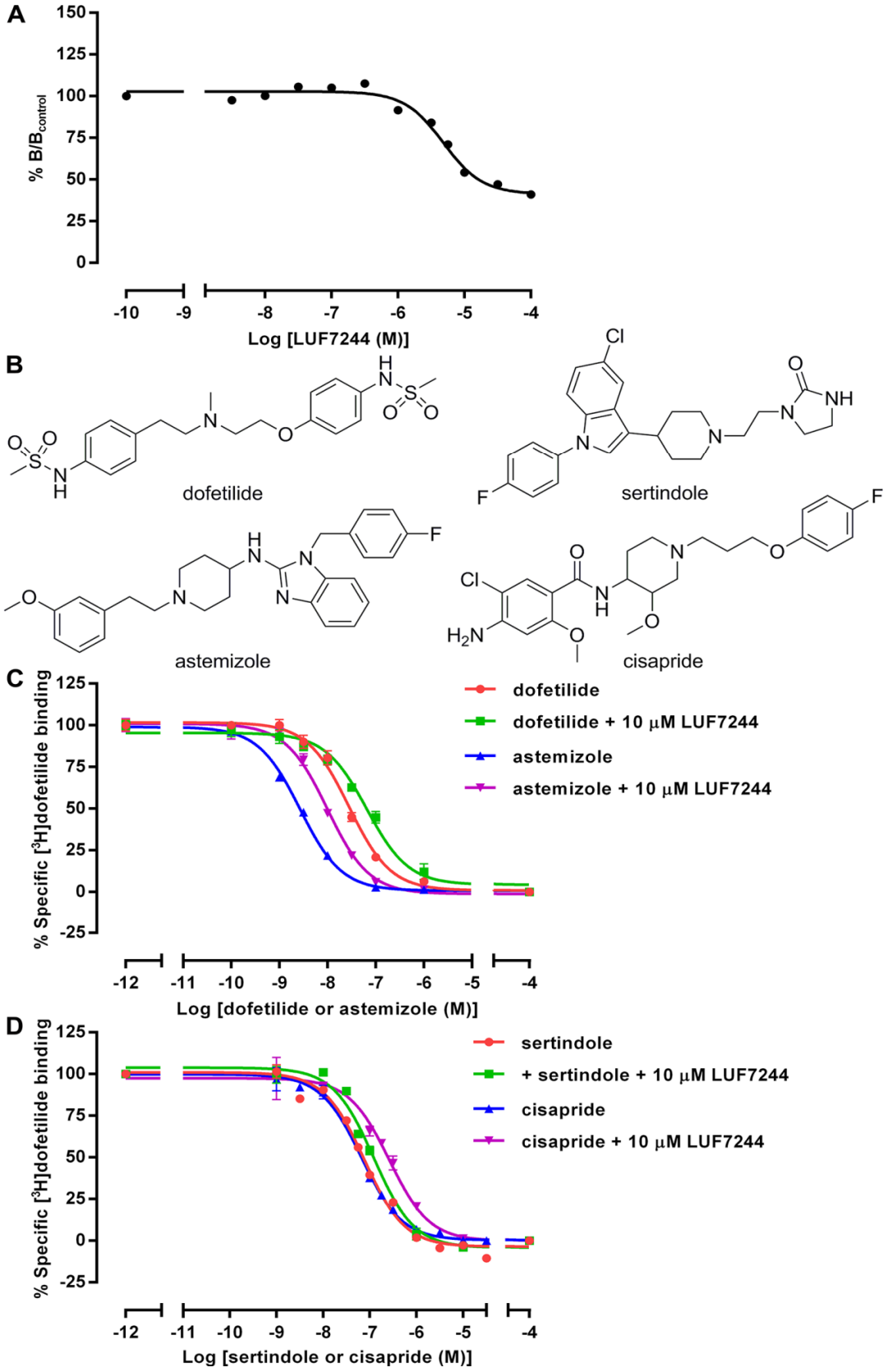

Figure 2. Assessment of the effects of LUF7244 on the binding of K_v11.1 blockers to the channel in a [^{3}H]dofetilide binding assay performed with membranes of HEK293K_v11.1 cells. A: Effect of different concentrations of LUF7244 on the dofetilide-induced dissociation of [^{3}H]dofetilide from the K_v11.1 channel. After preincubating HEK293K_v11.1 cell

membranes with [^{3}H]dofetilide, radioligand dissociation was induced by 10µM dofetilide in the absence or presence of different concentrations of LUF7244 and the incubation was terminated after 6 minutes. Results are expressed as the ratio of the specific binding of [^{3}H]dofetilide in the presence of 10µM dofetilide plus various concentrations of negative allosteric modulators (*B*) over that in the presence of 10µM dofetilide alone ($B_{control}$). B: Chemical structures of dofetilide, astemizole, sertindole and cisapride. C: Displacement curves of dofetilide and astemizole in the absence or presence of 10µM LUF7244. D: Displacement curves of sertindole and cisapride in the absence or presence of 10µM LUF7244.

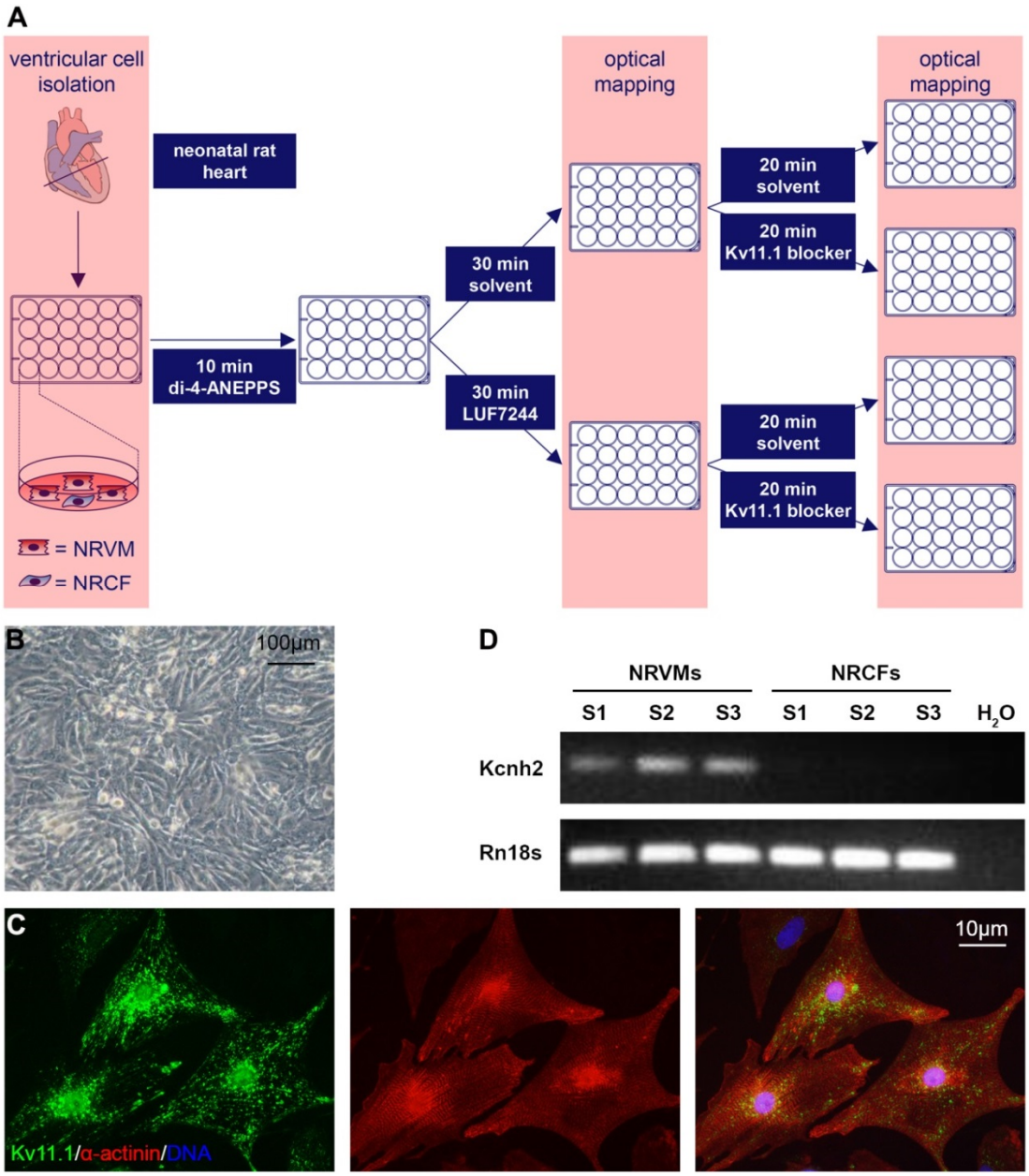

Figure 3. Biochemical characterization of the NRVM model. A: Basic setup of the optical voltage mapping experiments. **B:** Phase-contrast image of a typical confluent NRVM monolayer used for optical voltage mapping. **C:** Immunocytological analysis of K_v11.1 protein expression in NRVM cultures. The K_v11.1 protein (green) is mainly located around the nucleus (blue) and at the sarcolemma of the α-actinin (red)-positive NRVMs and hardly detectable in the α-actinin-negative non-cardiomyocytes. **D:** Analysis of *Kcnh2* mRNA levels in NRVMs and NRCFs by RT-PCR.

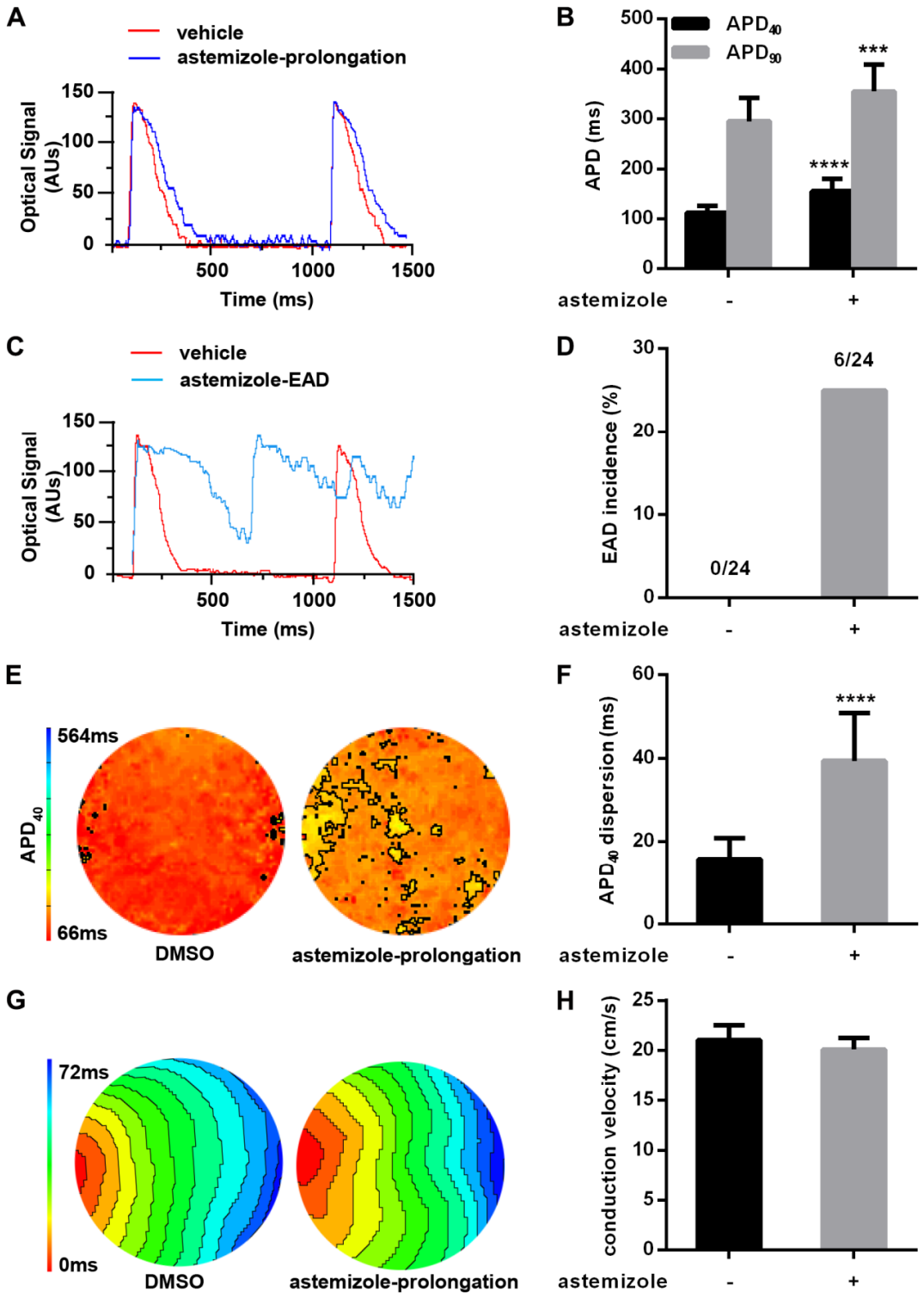

Figure 4. Electrophysiological characterization of the NRVM model by optical voltage mapping following 1-Hz electrical stimulation. Representative filtered optical signal traces (A and C), corresponding APD dispersion and activation maps (E and G, respectively) and quantitative analyses (bar graphs in B, D, F and H) of NRVM cultures exposed for 30 minutes to 100nM astemizole or vehicle (control) and subjected to optical voltage mapping immediately afterwards. Astemizole treatment resulted in APD prolongation (APD_{40} and APD_{90}, A and B), the occurrence of EADs (C and D) and an increase in APD_{40} dispersion (E and F) but did not significantly alter CV (G and H). ***P<0.001 and ****P<0.0001.

Electrophysiological Consequences of K_v11.1 Blockade by Astemizole in NRVMs
Due to its relatively high specificity for the K_v11.1 channel,[20] astemizole was selected to study the electrophysiological consequences of K_v11.1 blockade by optical voltage mapping (**Figure 4**). NRVMs treated with astemizole displayed a concentration-dependent increase in APD and EAD incidence (**Figure I** in the **Data Supplement**). As displayed in **Figure 4A-B**, APD_{40} and APD_{90} values of NRVMs were increased from 112±16 and 295±62ms in vehicle-treated cultures (n=24) to 156±39 and 355±66ms in cultures containing 100nM astemizole (n=24, $P<0.0001$ and $P<0.001$, respectively). Furthermore, exposure to 100nM astemizole resulted in the occurrence of EADs in 25% of the NRVM cultures, whereas no EADs were observed under control conditions (**Figure 4C-D**). As shown in **Figure 4E-F**, the APD_{40} dispersion between NRVMs in the presence of 100nM astemizole was significantly higher than that in its absence (39±11 vs 16±5ms; $P<0.0001$), indicative of aggravated repolarization heterogeneity due to inhibition of I_{Kr} by astemizole. Occasionally, the astemizole-induced APD prolongation resulted in short-lasting, irregular tachyarrhythmias (**Figure II** in the **Data Supplement**) reminiscent of spontaneously terminating TdP episodes. Importantly, as indicated by the activation maps (**Figure 4G**) and corresponding quantitative analysis (**Figure 4H**), the CV in NRVM cultures was not significantly influenced by 100nM astemizole (20±4cm/s vs 21±3cm/s in control cultures; P=0.1254). Collectively, these data validate the utility of NRVM cultures as an in-vitro model for investigating the AP-prolonging and associated proarrhythmic effects of K_v11.1 blockers like astemizole.

Effects of LUF7244 on K_v11.1 Blockade-Associated Proarrhythmic Changes in NRVM Cultures
To investigate the functional consequences of negative allosteric modulation of K_v11.1's interaction with typical K_v11.1 blockers, di-4-ANNEPS-loaded NRVM cultures were incubated for 20 minutes in culture medium containing 10μM LUF7244 before addition of astemizole, sertindole or cisapride. Since the K_i values of sertindole and cisapride for K_v11.1 are more than 10 times higher than that of astemizole (**Table II** in the **Data Supplement**), these drugs were tested at a final concentration of 1μM instead of 100nM as was used for astemizole. After incubation for 30 minutes, the NRVMs were optically mapped. As shown in **Figure 5A**, the APD-prolonging and EAD-promoting effects of astemizole were effectively suppressed by LUF7244. APD_{40} and APD_{90} were significantly shortened from 156±39ms to 118±18ms (n=24, $P<0.0001$) and from 355±66ms to 282±63ms (n=24, $P<0.001$), respectively, *i.e.*, LUF7244 was able to reduce APD_{40} and APD_{90} to control values (**Figure 5B**). Moreover, in the presence of 10μM LUF7244 EADs were no longer observed in NRVM cultures exposed to 100nM astemizole (**Figure 5C**). LUF7244 also prevented the increase in APD_{40} dispersion caused by astemizole (**Figure 5D-E**). Importantly, the CVs in NRVM cultures treated with vehicle, LUF7244, astemizole or LUF7244 plus astemizole did not significantly differ (data not shown). Also, at a final concentration of 10μM LUF7244 per se did not reduce APD or significantly affect APD_{40} dispersion (**Figure 5F-H** and **Figure III** in the **Data Supplement**), suggesting that this negative allosteric modulator poses very little, if any, risk for the development of arrhythmias associated with abnormal APD shortening. Very similar

results of LUF7244 were obtained in NRVM cultures exposed to sertindole or cisapride (**Figure IV** in the **Data Supplement**). LUF7244 can thus suppress the proarrhythmic side effects of drugs from different therapeutic classes by allosteric modulation of the $K_v11.1$ channel without exerting, by itself, any obvious adverse electrophysiological effects on cardiomyocytes.

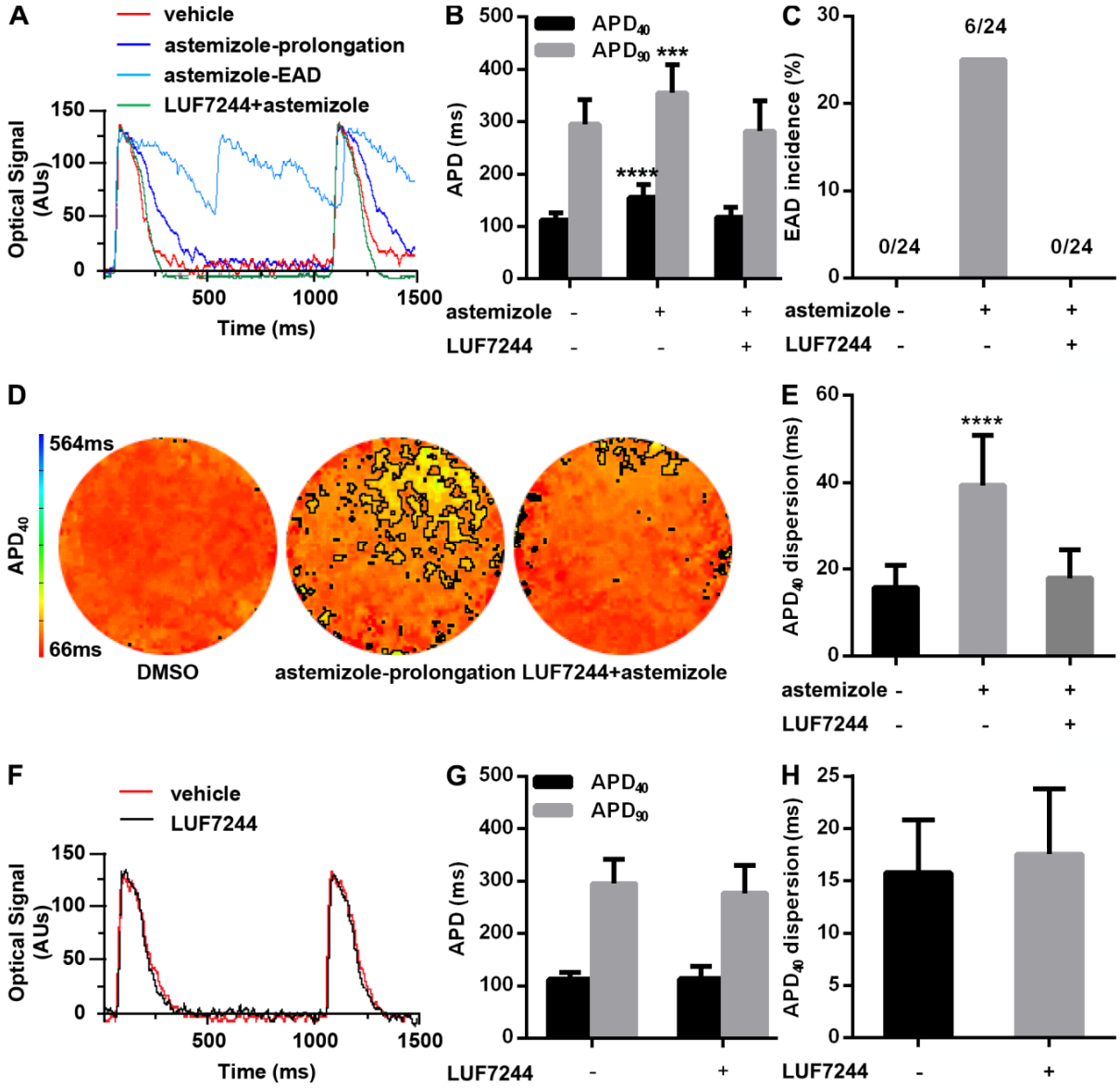

Figure 5. Assessment by optical voltage mapping of the ability of LUF7244 to counteract the proarrhythmic effects of astemizole on NRVMs. Representative filtered optical signal traces (A and F), APD dispersion maps (D) and quantitative analysis (bar graphs in B, C, E, G and H) of control NRVM cultures and of NRVM cultures that had been treated with 100nM astemizole or with 10µM LUF7244 followed by 100nM astemizole immediately before optical voltage mapping. Pretreatment of NRVM cultures with LUF7244 completely prevented the astemizole-induced APD prolongation (APD_{40} and APD_{90}; B), occurrence of EADs (C) and increase in APD_{40} dispersion (D and E). Treatment of NRVM cultures with 10µM LUF7244 only did not change AP morphology (F), APD (G) or APD_{40} dispersion (H). ***P<0.001 and ****P<0.0001.

Discussion

Major Findings

In radioligand binding assays the structurally related compounds VU0405601, ML-T531 and LUF7244 were found to weaken the interaction between the human $K_v11.1$ channel and the class III antiarrhythmic agent dofetilide as well as the unintended $K_v11.1$ blockers astemizole, sertindole and cisapride. VU405601, ML-T531 and LUF7244 exerted their negative effects on the binding of typical $K_v11.1$ blockers to the channel's central cavity by an allosteric mechanism. Importantly, LUF7244 decreased the $K_v11.1$ affinity of astemizole without influencing its affinity at the hH_1R, being astemizole's intentional target (**Figure V** in the **Data Supplement**). Optical voltage mapping showed that incubation of NRVM monolayers with astemizole, sertindole or cisapride led to a significant increase in APD, APD dispersion and, except for cisapride, EAD incidence demonstrating the usefulness of this cellular model system for studying $K_v11.1$ blockade-related proarrhythmic risk. Pretreatment of NRVMs with 10μM LUF7244 effectively prevented the proarrhythmic changes induced by astemizole, sertindole and cisapride without significantly shortening APD by itself and without adversely affecting NRVM viability, excitability and contractility (**Figure VI** in the **Data Supplement**). These findings provide a rationale for further exploring allosteric mo^{du}lation as a strategy to prevent DiVAs.

NRVM Monolayers as Model for Studying Drug-Induced LQTS

Many different methods have been exploited to assess drugs for their $K_v11.1$ blockade-associated arrhythmogenicity.[3,21] The interaction between a drug and the $K_v11.1$ channel is usually first investigated by computational and biochemical assays. Next, the $K_v11.1$ liabilities of suspicious drugs are typically evaluated by electrophysiological measurements on CHO or HEK293 cells expressing the human $K_v11.1$ channel. Despite their practical advantages, these non-excitable cellular models do not recapitulate the complex regulatory circuits governing $K_v11.1$ channel activity in cardiomyocytes and are unsuitable for studying AP generation and propagation. To overcome these shortcomings, human induced pluripotent stem cell-derived cardiomyocytes (hiPSC-CMs) are now often used for cardiotoxicological screenings.[22] However, thus far hiPSC-CMs cannot produce dense monolayers of phenotypically homogeneous ventricular cardiomyocytes for high-resolution optical mapping.[23] We hence employed NRVM monolayers to study the effects of LUF7244 on the proarrhythmic potential of three inadvertent $K_v11.1$ blockers by optical voltage mapping. The reasons to specifically use NRVMs for this purpose are that these cells (i) can be relatively easily isolated and cultured, (ii) are well-characterized and (iii) express functional $K_v11.1$ channels.[24] However, this is the first study using NRVMs to test compounds for their ability to prevent DiVAs resulting from unintended $K_v11.1$ blockade.

Although mechanistic insight into DiVAs is limited, there is broad consensus about spatial dispersion of repolarization and EAD-induced triggered activity providing the substrate and trigger for the genesis of drug-induced TdP, respectively.[2] The EADs typically arise during phase 2 of the cardiac AP due to drug-dependent decreases in I_{Kr} causing increases of APD and QT interval. In support of the validity

of our model, astemizole dose-dependently increased APD and EAD incidence in monolayers of NRVMs (**Figure I** in the **Data Supplement**). Also sertindole and cisapride had APD-prolonging effects (**Figure IVA** and **IVD** in the **Data Supplement**) and each of the three fortuitous $K_v11.1$ blockers increased APD dispersion (**Figure 4F**, **Figure IVC** and **IVF** in the **Data Supplement**). While 100nM astemizole, 1μM sertindole and 1μM cisapride increased APD and APD dispersion to a similar extent, cisapride did not significantly increase EAD incidence in contrast to the other two drugs (**Figure 4D**, **Figure IVB** and **IVE** in the **Data Supplement)**. This finding may be explained by cisapride's inhibitory effect on the $I_{Ca,L}$ in NRVMs.[25]

Initially, EAD-dependent ectopic activity at multiple competing foci was thought to generate the undulating electrocardiographic patterns of TdP. Recently, meandering $I_{Ca,L}$-mediated reentrant circuits initiated by EADs at single foci have been proposed as an alternative explanation for the highly characteristic electrocardiographic signature of TdP.[26,27] Although we did observe several instances of short-lasting, irregular tachyarrhythmias exclusively in NRVM cultures exposed to $K_v11.1$ blockers, they did not allow us to make specific claims about the underlying electrophysiological mechanisms. Pretreatment with LUF7244 rendered NRVM monolayers unsusceptible to the $K_v11.1$-blocking effects of astemizole, sertindole and cisapride. In the presence of LUF7244, these $K_v11.1$ blockers no longer caused heterogeneous APD prolongation and, due to the reduced opportunity for L-type Ca^{2+} channel reactivation, no longer gave rise to EADs. This raises the perspective to use LUF7244 as an antiarrhythmic additive to drugs with unintended I_{Kr}-suppressing effects. Thus, radioligand binding assays in combination with optical voltage mapping experiments of NRVM cultures offer convenient preclinical test systems for evaluating chemical entities that can potentially reduce $K_v11.1$-related cardiotoxicity.

LUF7244's Mode of Action

The chemical structure of LUF7244 resembles those of ML-T531 and VU0405601. In a recent study, 10μM of ML-T531 was shown to reduce the APD of hiPSC-CMs from an LQT1 patient to that of control cells by augmenting I_{Kr}.[11] However, the effects of ML-T531 on the APD of hiPSC-CMs from a healthy individual and ML-T531's ability to inhibit the APD-prolonging effects of unintended $K_v11.1$ blockers were not investigated. Voltage-clamp recordings of $K_v11.1$-expressing CHO cells showed that ML-T531 reduces the deactivation rate of the $K_v11.1$ channel and causes a shift of its inactivation curve towards more positive voltages. Shortly after the discovery of ML-T531, VU0405601 was identified as a compound that, at a final concentration of 5μM, protected Langendorff-perfused rabbit hearts from the proarrhythmic effects of exposure to 100nM dofetilide.[7] Although VU0405601 only partially reversed the dofetilide-dependent increase in APD, its administration prior to dofetilide strongly reduced the pacing-induced arrhythmia incidence from 42% to 4%, which was very close to the 2% of pacing-induced premature ventricular contractions observed in untreated hearts.[7] Exposure of isolated rabbit ventricular myocytes to 5μM of VU0405601 only marginally reduced APD, which is consonant with our finding that 10μM LUF7244 did not noticeably affect the APD of NRVMs. However, at a final concentration of 50μM, VU0405601 decreased the APD_{50} and APD_{90} of rabbit ventricular myocytes by 35±6% and 32±4%, respectively. Patch-clamp analysis of

HEK293K_v11.1 cells linked the APD-shortening effect of 50μM VU0405601 to shifts in the $V_{½}$ of activation and inactivation and to changes in the kinetics of (de)activation and (de)inactivation causing an increase in I_{Kr}.

In this study, we found that VU0405601, ML-T531 and LUF7244 displayed comparatively low K_v11.1 affinities with Hill coefficients significantly different from unity for their [^{3}H]dofetilide displacement curves. This suggests that these ligands bind to the K_v11.1 channel at sites distinct from that of dofetilide, indicative of an allosteric mode of action.[10,28,29] The binding of a drug to a receptor at an allosteric site (*i.e.*, a site topologically distinct from that of the test ligand) triggers a conformational change within the receptor ultimately causing an alteration of the ligand's dissociation rate from its cognate (*i.e.*, orthosteric) binding site.[10,30] Altered ligand dissociation rates have been found representative of allosteric interactions in various drug targets such as muscarinic and adenosine receptors.[10, 31-33] Consistently, VU0405601, ML-T531 and LUF7244 significantly accelerated the dissociation of dofetilide from the K_v11.1 channel, strengthening the conclusion that they are negative allosteric modulators of dofetilide binding to the K_v11.1 channel. Our finding for VU0405601 is in agreement with the results of Potet *et al.*, who presented indirect evidence that VU0405601 binds from outside to the ectodomain of the K_v11.1 channel,[7] while astemizole, cisapride, dofetilide and sertindole all bind to the channel's central cavity from inside.[34-36] In addition, the [^{3}H]dofetilide displacement curves of dofetilide, astemizole, sertindole and cisapride were shifted rightwards by LUF7244 (**Figure 2C-D**) providing further proof for its negative allosteric effect.[10,33] Collectively, the results of the different radioligand binding assays provide strong evidence that VU0405601, ML-T531 and LUF7244 are negative allosteric modulators of dofetilide binding to the K_v11.1 channel. Binding of VU0405601, ML-T531 and LUF7244 likely alters the 3D structure of the K_v11.1 channel, which decreases its affinity for typical K_v11.1 blockers by increasing the dissociation rates of these blockers from the channel. Notably, the vast majority of fortuitous K_v11.1 blockers exert their effects by occupying the central cavity of the K_v11.1 channel and thereby obstructing the transport of K^+ ions through the channel's pore.[37] There are, however, also examples of drugs that reduce I_{Kr} by inhibiting, directly or indirectly, the trafficking of K_v11.1 to the plasma membrane.[38] Given their specific mode of action, it is unlikely that the I_{Kr}-inhibiting effects of these drugs can be abolished by LUF7244 or a related compound.

The ability of LUF7244 to counteract astemizole-, sertindole- and cisapride-related arrythmogenesis may be the combined result of its inhibitory allosteric effect on the binding of these unintended K_v11.1 blockers to the channel and of its direct enhancing effect on the K_v11.1 channel's activity. Indeed, at concentrations ≥25μM, LUF7244 caused APD shortening (**Figure III** in the **Data Supplement**) suggesting that LUF7244 can directly act as (allosteric) K_v11.1 activator like VU0405601 and ML-T531.[7,11] However, the fact that exposure of NRVMs to 10μM LUF7244 alone did not significantly change AP characteristics suggests that LUF7244's K_v11.1-activating activity is not of critical importance for its ability to suppress the proarrhythmic effects of inadvertent K_v11.1 blockers. The absence of a noticeable change in AP shape and duration following exposure of NRVMs to 10μM LUF7244 also argues against a possible effect of this allosteric modulator on cardiac ion channels different from the K_v11.1 channel. In keeping with this notion, Na_v1.5 and

$K_v1.5$ currents and I_{Ks} were not affected or only slightly reduced by 50μM VU0405601.[7] Likewise, ML-T531 at a final concentration of 10μM had a minor suppressive effect on I_{Ks} and did not influence $Na_v1.5$, $Ca_v1.2$, $K_v4.3$ or Kir2.1 activities.[11] Thus, the antiarrhythmic propensity of LUF7244 is dominated by its negative allosteric impact on the binding of typical $K_v11.1$ blockers to the channel.

Since LUF7244 significantly decreased the $K_v11.1$ affinities of drugs with very different chemical structures (**Figure 2B**) in radioligand binding assays and prevented these drugs from causing APD prolongation in NRVMs, LUF7244 may be effective in reducing the cardiotoxicity of a broad range of $K_v11.1$ blockers. Further support for this notion comes from the fact that VU0405601, which was here shown to inhibit dofetilide's interaction with the $K_v11.1$ channel by a similar mechanism to LUF7244, could abolish the blockade of $K_v11.1$ by seven different drugs.[7] The different degree to which LUF7244 increased the K_i values of dofetilide, astemizole, sertindole and cisapride suggests that the sensitivity of different $K_v11.1$ blockers to conformational changes in the $K_v11.1$ proteins differs. Accordingly, different LUF7244 concentrations may be required to abrogate the proarrhythmic effects of distinct $K_v11.1$ blockers.

Although at a final concentration of 50μM LUF7244's ability to weaken the interaction between [^{3}H]dofetilide and the $K_v11.1$ channel was similar to those of VU0405601 and ML-T531 (**Figure 1D**), the new modulator was much more effective than the other two compounds at a final concentration of 10μM (**Figure 1C**). Moreover, even 50μM VU0405601 only modestly inhibited the APD-prolonging effect of 1μM dofetilide (K_i for human $K_v11.1$: 6.0nM) on rabbit ventricular myocytes,[7] while 10μM LUF7244 totally blocked the APD prolongation caused by exposure of NRVMs to 100nM astemizole (K_i for human $K_v11.1$: 1.2nM). These findings together with the substantial decrease in the APD of normal rabbit ventricular myocytes caused by 50μM VU0405601 (see above), suggests that LUF7244 may possess a more favorable safety profile than VU0405601 or ML-T531.

Limitations

Due to the difficulty to obtain and culture adult human ventricular myocytes, NRVMs were used as 2D model system to investigate the effects of LUF7244 on $K_v11.1$ blockade-associated proarrhythmic changes in cardiac electrophysiology. However, ventricular adult human and neonatal rat cardiomyocytes have different AP morphologies because of qualitative and quantitative differences in the molecular components shaping the APs. Also, changes in cardiomyocyte electrophysiological properties may work out differently in a 2D cell layer than in the (3D) heart. Nonetheless, studies on NRVM monolayers have greatly contributed to our current understanding of cardiac electrophysiology. Moreover, in spite of the differences in ventricular ion channel composition between humans and rats, their $K_v11.1$ proteins are very similar showing 95% amino acid identity for the largest isoforms. Consistently, the results of the radioligand binding assays, which were carried out with the human $K_v11.1$ protein, correlated very well with those of the optical mapping studies using NRVMs. Yet, ultimately, the ability of LUF7244 to counteract the proarrhythmic effects of unintended $K_v11.1$ blockers should be investigated in human subjects.

As mentioned above, LUF7244 did not inhibit the binding of astemizole to its intended target in radioligand binding assays (**Figure V** in the **Data Supplement**) and did not compromise the viability, excitability or contractility of NRVMs (**Figure VI** in the **Data Supplement**) at a concentration sufficient to fully abrogate the proarrhythmic consequences of drug-induced $K_v11.1$ blockade in these cells. Despite these encouraging results, certainty about the lack of specific adverse/interfering effects of this negative allosteric modulator of $K_v11.1$ channel in humans can only be obtained through clinical studies. Moreover, now that the ability of LUF7244 to reduce the channel binding affinities of $K_v11.1$ blockers has been established, allosteric modulators with higher safety and/or efficacy than LUF7244 are likely to arise in the near future. The design of such compounds may benefit from identification of the precise binding site of LUF7244 at the $K_v11.1$ channel.

Conclusions

Allosteric modulators of the $K_v11.1$ channel could provide a new pharmacological treatment for drug-induced LQTS by preventing the potentially arrhythmogenic changes in AP characteristics caused by unintended $K_v11.1$ blockers. Through combined administration with a negative allosteric modulator, use of "old" drugs that have been banned because of their "$K_v11.1$ liabilities" may be resumed and new drugs with $K_v11.1$-blocking effects may not have to be excluded from clinical application.

Acknowledgements

We thank Cindy Schutte-Bart (Department of Cardiology, Leiden University Medical Center, Leiden, the Netherlands) for her help with establishing primary NRVM cultures and Prof. Guang-Qian Zhou (Anti-Ageing and Regenerative Medicine Centre, Shenzhen University, Shenzhen, People's Republic of China) for his efforts to establish collaborations between Dutch and Chinese researchers.

Funding Sources

Zhiyi Yu and Jia Liu were supported by the Chinese Scholarship Council. Additional support was provided by ICIN-Netherlands Heart Institute and the Royal Netherlands Academy of Arts and Sciences (Chinese Exchange Programme grant 10CDP007 to Antoine de Vries).

Disclosures

None.

References

1. Stockbridge N, Morganroth J, Shah RR, Garnett C. Dealing with global safety issues. Drug Saf. 2013;36:167-182.
2. Antzelevitch C. Ionic, molecular, and cellular bases of QT-interval prolongation and Torsade de Pointes. Europace. 2007;9:iv4-iv15.
3. Kannankeril P, Roden DM, Darbar D. Drug-induced long QT syndrome. Pharmacol Rev. 2010;62:760-781.
4. Vandenberg JI, Perry MD, Perrin MJ, Mann SA, Ke Y, Hill AP. hERG K^+ channels: Structure, function, and clinical significance. Physiol Rev. 2012;92:1393-1478.
5. Sanguinetti MC. hERG1 channel agonists and cardiac arrhythmia. Curr Opin Pharmacol. 2014;15:22-27.
6. Kang J, Chen X-L, Wang H, Ji J, Cheng H, Incardona J, Reynolds W, Viviani F, Tabart M, Rampe D. Discovery of a small molecule activator of the human ether-a-go-go-related gene (hERG) cardiac K^+ channel. Mol Pharmacol. 2005;67:827-836.
7. Potet F, Lorinc AN, Chaigne S, Hopkins CR, Venkataraman R, Stepanovic SZ, Lewis LM, Days E, Sidorov VY, Engers DW, Zou B, Afshartous D, George AL Jr, Campbell CM, Balser JR, Li M, Baudenbacher FJ, Lindsley CW, Weaver CD, Kupershmidt S. Identification and characterization of a compound that protects cardiac tissue from human ether-a-go-go-related gene (hERG)-related drug-induced arrhythmias. J Biol Chem. 2012;287:39613-39625.
8. May LT, Leach K, Sexton PM, Christopoulos A. Allosteric modulation of G protein-coupled receptors. Annu Rev Pharmacol Toxicol. 2007;47:1-51.
9. Conn PJ, Christopoulos A, Lindsley CW. Allosteric modulators of GPCRs: A novel approach for the treatment of CNS disorders. Nat Rev Drug Discov. 2009;8:41-54.
10. Christopoulos A, Changeux JP, Catterall WA, Fabbro D, Burris TP, Cidlowski JA, Olsen RW, Peters JA, Neubig RR, Pin J-P, Sexton PM, Kenakin TP, Ehlert FJ, Spedding M, Langmead CJ. International union of basic and clinical pharmacology. Xc. Multisite pharmacology: Recommendations for the nomenclature of receptor allosterism and allosteric ligands. Pharmacol Rev. 2014;66:918-947.
11. Zhang H, Zou B, Yu H, Moretti A, Wang X, Yan W, Babcock JJ, Bellin M, McManus OB, Tomaselli G, Nan F, Laugwitz KL, Li M. Modulation of hERG potassium channel gating normalizes action potential duration prolonged by dysfunctional KCNQ1 potassium channel. Proc Natl Acad Sci U S A. 2012;109:11866-11871.
12. Diaz GJ, Daniell K, Leitza ST, Martin RL, Su Z, McDermott JS, Cox BF, Gintant GA. The [^{3}H]dofetilide binding assay is a predictive screening tool for hERG blockade and proarrhythmia: Comparison of intact cell and membrane preparations and effects of altering $[K^+]_o$. J Pharmacol Toxicol Methods. 2004;50:187-199.
13. Ficker E, Jarolimek W, Kiehn J, Baumann A, Brown AM. Molecular determinants of dofetilide block of hERG K^+ channels. Circ Res. 1998;82:386-395.
14. Aronov AM. Predictive in silico modeling for hERG channel blockers. Drug Discov Today. 2005;10:149-155.
15. Yu Z, Klaasse E, Heitman LH, IJzerman AP. Allosteric modulators of the hERG K^+ channel: Radioligand binding assays reveal allosteric characteristics of dofetilide analogs. Toxicol Appl Pharmacol. 2014;274:78-86.

16. Pijnappels DA, Schalij MJ, Ramkisoensing AA, van Tuyn J, de Vries AA, van der Laarse A, Ypey DL, Atsma DE. Forced alignment of mesenchymal stem cells undergoing cardiomyogenic differentiation affects functional integration with cardiomyocyte cultures. Circ Res. 2008;103:167-176.
17. Askar SF, Ramkisoensing AA, Schalij MJ, Bingen BO, Swildens J, van der Laarse A, Atsma DE, de Vries AA, Ypey DL, Pijnappels DA. Antiproliferative treatment of myofibroblasts prevents arrhythmias in-vitro by limiting myofibroblast-induced depolarization. Cardiovasc Res. 2011;90:295-304.
18. Yu Z, IJzerman A, Heitman L. K_v11.1 (hERG)-induced cardiotoxicity: A molecular insight from a binding kinetics study of prototypic K_v11.1 (hERG) inhibitors. Br J Pharmacol. 2015;172:940-945.
19. Himel HD, Bub G, Lakireddy P, El-Sherif N. Optical imaging of arrhythmias in the cardiomyocyte monolayer. Heart Rhythm. 2012;9:2077-2082.
20. Redfern W, Carlsson L, Davis A, Lynch W, MacKenzie I, Palethorpe S, Siegl P, Strang I, Sullivan A, Wallis R, Camm AJ, Hammond TG. Relationships between preclinical cardiac electrophysiology, clinical QT interval prolongation and Torsade de Pointes for a broad range of drugs: Evidence for a provisional safety margin in drug development. Cardiovasc Res. 2003;58:32-45.
21. Heijman J, Voigt N, Carlsson LG, Dobrev D. Cardiac safety assays. Curr Opin Pharmacol. 2014;15:16-21.
22. Khan JM, Lyon AR, Harding SE. The case for induced pluripotent stem cell-derived cardiomyocytes in pharmacological screening. Br J Pharmacol. 2013;169:304-317.
23. Lee P, Klos M, Bollensdorff C, Hou L, Ewart P, Kamp TJ, Zhang J, Bizy A, Guerrero-Serna G, Kohl P, Jalife J, Herron TJ. Simultaneous voltage and calcium mapping of genetically purified human induced pluripotent stem cell-derived cardiac myocyte monolayers. Circ Res. 2012;110:1556-1563.
24. Korhonen T, Hänninen SL, Tavi P. Model of excitation-contraction coupling of rat neonatal ventricular myocytes. Biophys J. 2009;96:1189-1209.
25. Davie C, Pierre-Valentin J, Pollard C, Standen N, Mitcheson J, Alexander P, Thong B. Comparative pharmacology of guinea pig cardiac myocyte and cloned hERG (I_{Kr}) channel. J Cardiovasc Electrophysiol. 2004;15:1302-1309.
26. Murakawa Y. Focal and reentrant mechanisms of Torsades de Pointes: EAD, reentry, or chimera? J Arrhythm. 2011;27:28-37.
27. Chang MG, Sato D, de Lange E, Lee J-H, Karagueuzian HS, Garfinkel A, Weiss JN, Qu Z. Bi-stable wave propagation and early afterdepolarization-mediated cardiac arrhythmias. Heart Rhythm. 2012;9:115-122.
28. Pedigo N, Yamamura H, Nelson DL. Discrimination of multiple [^{3}H]5-hydroxytryptamine binding sites by the neuroleptic spiperone in rat brain. J Neurochem. 1981;36:220-226.
29. van den Nieuwendijk AM, Pietra D, Heitman L, Göblyös A, IJzerman AP. Synthesis and biological evaluation of 2,3,5-substituted [1,2,4] thiadiazoles as allosteric modulators of adenosine receptors. J Med Chem. 2004;47:663-672.
30. Vauquelin G, Van Liefde I. Radioligand dissociation measurements: Potential interference of rebinding and allosteric mechanisms and physiological relevance of the biological model systems. Expert Opin Drug Discov. 2012;7:583-595.

31. Schober DA, Croy CH, Xiao H, Christopoulos A, Felder CC. Development of a radioligand, [^{3}H]ly2119620, to probe the human M_2 and M_4 muscarinic receptor allosteric binding sites. Mol Pharmacol. 2014;86:116-123.
32. Gao Z, Van Muijlwijk-Koezen JE, Chen A, Müller CE, IJzerman AP, Jacobson KA. Allosteric modulation of A_3 adenosine receptors by a series of 3-(2-pyridinyl) isoquinoline derivatives. Mol Pharmacol. 2001;60:1057-1063.
33. Dror RO, Green HF, Valant C, Borhani DW, Valcourt JR, Pan AC, Arlow DH, Canals M, Lane JR, Rahmani R, Baell JB, Sexton PM, Christopoulos A, Shaw DE. Structural basis for modulation of a G-protein-coupled receptor by allosteric drugs. Nature. 2013;503:295-299.
34. Kamiya K, Niwa R, Mitcheson JS, Sanguinetti MC. Molecular determinants of hERG channel block. Mol Pharmacol. 2006;69:1709-1716.
35. Pearlstein RA, Vaz RJ, Kang J, Chen X-L, Preobrazhenskaya M, Shchekotikhin AE, Korolev AM, Lysenkova LN, Miroshnikova OV, Hendrix J, Rampe D. Characterization of hERG potassium channel inhibition using comsia 3D QSAR and homology modeling approaches. Bioorg Med Chem Lett. 2003;13:1829-1835.
36. García-Ferreiro RE, Kerschensteiner D, Major F, Monje F, Stühmer W, Pardo LA. Mechanism of block of hERG1 K^+ channels by imipramine and astemizole. J Gen Physiol. 2004;124:301-317.
37. Perry M, Stansfeld PJ, Leaney J, Wood C, de Groot MJ, Leishman D, Sutcliffe MJ, Mitcheson JS. Drug binding interactions in the inner cavity of hERG channels: Molecular insights from structure-activity relationships of clofilium and ibutilide analogs. Mol Pharmacol. 2006;69:509-519.
38. Nogawa H, Kawai T. hERG trafficking inhibition in drug-induced lethal cardiac arrhythmia. Eur J Pharmacol. 2014;741:336-339.

SUPPLEMENTAL MATERIAL

Materials

Dofetilide was synthesized in-house as previously described.[1] Bovine serum albumin (BSA, fraction V) and the fortuitous K_v11.1 blockers astemizole, sertindole and cisapride were purchased from Sigma-Aldrich (St. Louis, MO). Tritium-labeled dofetilide (specific activity: 82.3 Ci/mmol) and astemizole (specific activity: 78.4 Ci/mmol) were obtained from PerkinElmer (Groningen, the Netherlands). The synthesis and chemical analysis of VU0405601, ML-T531, as well as the design, synthesis and chemical analysis of LUF7244 will be detailed elsewhere. G418 was purchased from Stratagene (Cedar Creek, TX). All other chemicals were of analytical grade and obtained from standard commercial sources. HEK293K_v11.1 cells, *i.e.*, HEK293 cells stably overexpressing the human *KCNH2* gene, were kindly provided by Dr. Eckhard Ficker (Case Western Reserve University, Cleveland, OH).[2] Plasmid pcDNA3.1-hH_1Rwt encoding the human histamine H_1 receptor (hH_1R) was a gift of Prof. Thue W. Schwartz (University of Copenhagen, Copenhagen, Denmark). This plasmid was used to generate HEK293hH_1R cells, *i.e.*, cells transiently overexpressing the human *HRH1* gene (see "*HEK293 Cell Culture and Transfection*").

All animal experiments were approved by the Animal Experiments Committee of Leiden University Medical Center and conformed to the Guide for the Care and Use of Laboratory Animals as stated by the US National Institutes of Health.

Methods

HEK293 Cell Culture and Transfection

HEK293 cells were cultured in a humidified atmosphere at 37°C and 7% CO_2 in Dulbecco's modified Eagle's medium (DMEM; Sigma-Aldrich, catalog number: D6546) supplemented with 10% fetal bovine serum (Sarstedt, Nümbrecht, Germany), 50 IU/mL penicillin (Sarstedt) and 50 µg/mL streptomycin (Sarstedt). When the cells had reached 50-60% confluence, the culture medium was refreshed and 500 µL of 150 mM NaCl containing 15 µg of pcDNA3.1-hH_1Rwt DNA and 45 µg of linear 25-kDa polyethylenimine (Polysciences Europe, Eppelheim, Germany) was added per 100-mm culture dish (Sarstedt). The resulting HEK293hH_1R cells were harvested 48 hours after transfection.

Preparation of Membrane Samples

HEK293K_v11.1 cells were cultured and membranes were prepared and stored as detailed previously.[3] Membranes of HEK293hH_1R cells, were prepared and stored as described for HEK293K_v11.1 cells except that incubation buffer I (50 mM Tris-HCl [pH 7.4]) was used instead of incubation buffer II (10 mM HEPES-NaOH [pH 7.4], 130 mM NaCl, 60 mM KCl, 0.8 mM $MgCl_2$, 1 mM EGTA, 10 mM glucose, 0.1% BSA).

Radioligand Displacement Assays with [^{3}H]dofetilide

[^{3}H]Dofetilide binding assays for the K_v11.1 channel were performed in incubation buffer II as described previously.[3] Briefly, membrane aliquots containing 20 µg

protein were incubated with 5 nM [^{3}H]dofetilide in a total volume of 100 µL at 25°C for 1 hour. Radioligand displacement experiments were carried out with various concentrations of the test compounds. Total binding was determined in the presence of unsupplemented incubation buffer II, whereas non-specific binding was evaluated in incubation buffer II containing 10 µM astemizole. Displacement experiments with different concentrations of dofetilide, astemizole, sertindole and cisapride were conducted in the absence (control) or presence of 10 µM LUF7244. Incubations were terminated by dilution with ice-cold wash buffer (25 mM Tris-HCl [pH 7.4], 130 mM NaCl, 60 mM KCl, 0.8 mM $MgCl_2$, 0.05 mM $CaCl_2$, 0.05% BSA). Free radioligand was separated from bound [^{3}H]dofetilide by rapid filtration through a UniFilter-96 GF/B microplate using a PerkinElmer MicroBeta Filtermate-96 harvester. The filter-bound radioactivity was determined using a Wallac 1450 MicroBeta TriLux liquid scintillation counter (PerkinElmer) after extraction with 25 µL MicroScint 20 (PerkinElmer).

Radioligand Displacement Assays with [^{3}H]astemizole

[^{3}H]Astemizole binding assays for the hH_1R were performed in incubation buffer I. Membrane aliquots containing 15 µg protein were incubated with 3.5 nM [^{3}H]astemizole in a total volume of 100 µL at 25°C for 3 hours. Total binding was determined in the presence of unsupplemented incubation buffer I, whereas non-specific binding was evaluated in incubation buffer I containing 100 µM astemizole. LUF7244 displacement assays were carried out with various concentrations of this compound, while displacement assays with different concentrations of astemizole were conducted in the absence (control) or presence of 10 µM LUF7244. Incubations were terminated by dilution with ice-cold wash buffer (50 mM Tris-HCl [pH 7.4]). Samples were processed further as described under "*Radioligand Displacement Assays with [^{3}H]dofetilide*".

Kinetic Dissociation Assays with [^{3}H]dofetilide

Kinetic dissociation assays of [^{3}H]dofetilide were performed as described previously[3] with the following modifications. Single-point dissociation experiments were conducted by addition of 10 µM dofetilide in the absence (control) or presence of 10 or 50 µM of the selected compounds after preincubating membranes with [^{3}H]dofetilide at 25°C for 2 hours. After 6 minutes of dissociation, incubations were terminated and samples were obtained as described under "*Radioligand Displacement Assays with [^{3}H]dofetilide*". Traditional dissociation experiments were carried out with 10 µM dofetilide in the absence (control) or presence of 50 µM of the test compounds at 25°C for a total period of 2 hours after preincubation with the radioligand. The amounts of [^{3}H]dofetilide still bound to the receptor were measured at various time intervals. The concentration-dependent effect of LUF7244 was determined by addition of 10 µM dofetilide in the absence (control) or presence of different concentrations of LUF7244. After 6 minutes of dissociation, incubations were terminated and samples were obtained as described under "*Radioligand Displacement Assays with [^{3}H]dofetilide*". The non-radiolabeled dofetilide was applied at a concentration 1667-fold higher than the K_i for the interaction of dofetilide

with $K_v11.1$ (**Table II**), to avoid a significant contribution of reassociation of the radioligand with the channel to the results of the kinetic dissociation assays.

Isolation and Culture of Neonatal Rat Ventricular Myocytes (NRVMs)

NRVMs were isolated and cultured as described previously.[4] Briefly, neonatal rats were anaesthetized with 4-5% isoflurane inhalation anesthesia. After adequate anesthesia had been confirmed by the absence of reflexes, the heart was quickly excised. Ventricles were separated from the remainder of the heart, cut into small pieces with a fine scissor and a scalpel and dissociated by collagenase type l (Worthington, Lakewood, NJ) digestion. The resulting cell suspension was applied to Primaria culture dishes (Corning Life Sciences, Amsterdam, the Netherlands) and incubated for 75 minutes at 37°C in a humidified atmosphere of 5% CO_2 to allow preferential attachment of cardiac fibroblasts. The unattached cells (mainly cardiomyocytes) were collected, passed through a cell strainer (70-µm mesh pore size; BD Biosciences, Breda, the Netherlands) and applied at a density of 8×10^5 cells/well of a 24-well cell culture plate (Corning Life Sciences) to fibronectin (Sigma-Aldrich)-coated, round glass coverslips. Proliferation of residual cardiac fibroblasts (10-15%) was inhibited by incubating the cells for 2 hours in culture medium containing 10 µg/mL mitomycin C (Sigma-Aldrich) at 24 hours after seeding (*i.e.*, at day 1 of culture). Cells were subsequently maintained in a 1:1 mixture of DMEM (Life Technologies Europe, Bleiswijk, the Netherlands, catalog number: 22320) and Ham's F10 medium (Life Technologies Europe, catalog number: 11550) supplemented with 5% horse serum (Life Technologies Europe), 2% BSA and sodium ascorbate to a final concentration of 0.4 mM. This so-called NRVM medium was replaced daily.

Immunocytochemical Analyses

NRVMs were plated on fibronectin-coated, 15-mm diameter round glass coverslips at a density of 4×10^4 cells. At day 9 of culture, the cells were washed thrice with ice-cold phosphate-buffered saline (PBS), fixed for 30 minutes in buffered 4% formaldehyde (Added Pharma, Oss, the Netherlands) of 4°C and permeabilized by a 10-minute incubation at room temperature (RT) with 0.1% Triton X-100 in PBS. Next, the cells were double-immunostained for $K_v11.1$ (rabbit polyclonal antibodies raised against the C terminus of human $K_v11.1$, Merck Millipore, Billerica, MA, catalog number: AB5930) and α-actinin (mouse monoclonal antibody, Sigma-Aldrich, clone: EA-53). Incubation with primary antibodies (diluted 1:200 in PBS-0.1% normal donkey serum) and corresponding donkey Alexa Fluor 488/568-conjugated secondary antibodies (1:400 dilution, Life Technologies Europe) lasted for 2 hours. To visualize their nuclei, the cells were incubated for 10 minutes at RT with 10 µg/mL Hoechst 33342 (Life Technologies Europe) in PBS. After each processing step, the cells were washed three times with PBS of RT. To minimize photobleaching, coverslips were mounted in VECTASHIELD mounting medium (Vector Laboratories, Burlingame, CA). Photomicrographs were obtained with the aid of a digital color camera-equipped fluorescence microscope (Nikon Eclipse 80i; Nikon Instruments Europe, Amstelveen, the Netherlands).

Reverse Transcription-Quantitative Polymerase Chain Reaction Analyses

Cultures of NRVMs and of neonatal rat cardiac fibroblasts (NRCFs; maintained in NRVM medium) were washed once with ice-cold PBS after which the cells were lysed in TRIzol reagent (Life Technologies Europe) and total RNA was isolated using the RNeasy Mini kit (QIAGEN Benelux, Venlo, the Netherlands). The RNA was reverse transcribed with the iScript cDNA synthesis kit (Bio-Rad, Hercules, CA) and the resulting cDNA was amplified by PCR using the Bioline SensiFAST SYBR No-ROX kit (GC biotech, Alphen aan den Rijn, the Netherlands). The forward and reverse primers for the amplification of rat *Kcnh2*-specific cDNA were localized in different exons and had the following sequences, respectively: 5′ TAGCCTCCTCAACATCCC 3′ and 5′ CCATGTCTGCACTTAGCC 3′. For normalization purposes, rat 18S rRNA (*Rn18s*)-specific cDNA was amplified in parallel using the following forward and reverse primer, respectively: 5' GTAACCCGTTGAACCCCATT 3' and 5' CCATCCAATCGGTAGTAGCG 3'. PCR amplifications were carried out in a CFX96 Touch Real-Time PCR detection system (Bio-Rad) using a 2-step cycling protocol (20-40 cycles of 95°C 10 sec, 60°C 30 sec) after a 5-minute incubation at 95°C. Quantitative analyses were based on the $2^{-\Delta\Delta CT}$ method using CFX Manager software (Bio-Rad). For these analyses, PCRs were performed *in triplo* on three independent samples.

Optical Voltage Mapping

Action potentials (APs) were investigated on a whole-culture scale by optical voltage mapping using the potentiometric dye di-4-ANEPPS (Life Technologies Europe) as described previously.[5] The measurements were carried out at 37°C on 9-day-old confluent NRVM monolayer cultures (**Figure 3B** in the **Main Manuscript**). Optical signals were captured using a MiCAM ULTIMA-L imaging system (SciMedia, Costa Mesa, CA). To validate the experimental model, cells were incubated for 20 minutes in culture medium containing 0, 10, 30, 100 or 300 nM of the hH_1R antagonist and unintended $K_v11.1$ blocker astemizole and dimethylsulfoxide (DMSO) at a final concentration of 0.03%. In a subsequent experiment, NRVM cultures were first exposed for 30 minutes to 10 μM LUF7244 or its solvent (*i.e.*, culture medium containing 0.1% DMSO). Next, astemizole (final concentration of 100 nM) or vehicle was added to the culture medium raising the DMSO concentration to 0.13%. Following an incubation period of 30 minutes at 37°C, optical recordings were started in the continued presence of the appropriate vehicle/drug combinations (see **Figure 3A** in the **Main Manuscript** for a scheme of the basic experimental setup). Optical traces were analyzed using Brain Vision Analyzer 1208 software (Brainvision, Tokyo, Japan). To minimize noise artifacts, calculations were based on the average of the signals at a selected pixel and its eight nearest neighbors. Conduction velocity (CV), AP duration (APD) at 40 and 90% repolarization (APD_{40} and APD_{90}, respectively), APD dispersion and early afterdepolarizations (EADs) incidence were determined using NRVM cultures showing uniform AP propagation and 1:1 capture after 1-Hz local stimulation. Each of these electrophysiological parameters was the average of values obtained from 6 different positions equally distributed across the cell cultures.

The effects of LUF7244 on the $K_v11.1$-inhibiting antipsychotic drug sertindole and gastroprokinetic agent cisapride were assessed in the same way as for astemizole expect that the final concentration of sertindole and cisapride was 1 μM.

To study the effects of long-term $K_v11.1$ allosteric modulation in the absence and presence of an unintended $K_v11.1$ blocker on cardiac excitability, confluent NRVM cultures were incubated for 3 days in culture medium containing 100 nM astemizole and/or 10 μM LUF7244 prior to potentiometric dye loading, short-term drug treatment (see above) and optical mapping in the continued presence of drug(s) at culture day 9. Confluent NRVM monolayers exposed to culture medium containing vehicle (*i.e.*, DMSO at a final concentration of 0.13%) only, served as negative controls for this experiment. Just prior to optical mapping, movies of the cells were made using a Carl Zeiss Axiovert 40C microscope equipped with a LD A-Plan 20×/0.3 Ph1 objective (Zeiss Nederland, Sliedrecht, the Netherlands) to record their contractions upon electrical field stimulation using two epoxy-coated platinum electrodes with an interelectrode spacing of 13 mm. The electrical stimulus consisted of a 1.5-ms rectangular pulse of 12V produced at a frequency of 1 Hz by a model EV4543 miniature temporary cardiac pacemaker (PACE Medical, Waltham, MA).

Apoptosis Assay

To investigate the effects of long-term $K_v11.1$ allosteric modulation in the absence or presence of simultaneous $K_v11.1$ blockade on cell viability, externalized phosphatidylserine (as early marker of apoptosis) was detected using Alexa Fluor-568-conjugated annexin V (Life Technologies Europe). NRVM cultures in 24-well plates were treated cells for 72 hours with 100 nM astemizole and/or 10 μM LUF7244 as described under *"Optical Voltage Mapping"*. Mock-treated cells and cells incubated for 24 hours in culture medium containing 1 μM doxorubicin (Sigma-Aldrich) served as negative and positive controls, respectively. Next, the cells were washed once with ice-cold PBS and incubated for 15 minutes at RT with annexin V conjugate diluted 40-fold in binding buffer (10 mM HEPES-NaOH [pH 7.4], 140 mM NaCl, 2.5 mM $CaCl_2$) of 4°C containing 10 μg/mL Hoechst 33342. After a single wash with binding buffer of 4°C, photomicrographs were taken using a Leica DMI6000 B inverted microscope equipped with a Leica DFC300 FX digital color camera (both from Leica Microsystems, Rijswijk, the Netherlands).

Data Analysis

Data of the radioligand binding assays were analyzed with GraphPad Prism 5.0 (GraphPad Software, San Diego, CA). Half maximal inhibitory concentrations (*i.e.*, IC_{50} values) in displacement assays were directly obtained from non-linear regression analysis of dose-response curves. Half maximal inhibitory concentrations (*i.e.*, IC50 values) in displacement assays were directly obtained from non-linear regression analysis of dose-response relationships by four-parameter logistic curve fitting. Apparent inhibitory binding constants (K_i values) were derived from the IC_{50} values according to the Cheng-Prusoff relationship[6]: $K_i=IC_{50}/(1+[L^*]/K_D)$, where [L*] is the concentration of radioligand and K_D is its dissociation constant determined by saturation assay[7]. Dissociation rate constants (k_{off}) were obtained by computer analysis of the exponential decay of [^{3}H]dofetilide bound to the $K_v11.1$ channel. Half maximal effective concentrations (*i.e.*, EC_{50} values) from kinetic dissociation assays were calculated by non-linear regression analysis of concentration-effect curves of dissociation in the presence of different concentrations of unlabeled ligands. Values

obtained from the radioligand binding assays are means of three independent experiments performed in duplicate. The number of samples per experimental group in the optical voltage mapping experiments varied from 6 to 24 as indicated. Data are expressed as mean±standard error of the mean (SEM) for the radioligand binding assays or as mean±standard deviation (SD) for the optical voltage mapping experiments. Statistical analysis of all the results were done using non-parametric tests, Mann-Whitney U test for comparison of two groups and Kruskal-Wallis test for comparison of more than two groups. Statistical analysis of the results of radioligand binding assays was done using nonparametric Mann-Whitney U test.

Supplemental Results

Comparison of the Concentration-dependent Effects of LUF7244 and VU0405601 on APD in NRVMs

Given the known APD-shortening effect of VU0405601[8] in rabbit ventricular cardiomyocytes and the similarities in chemical structure between LUF7244 and VU0405601, a side-by-side comparison of the concentration-dependent effects of these 2 compounds on the APD of NRVMs was performed. Consistent with the results shown in **Figure 5F and 5G** of the **Main Manuscript**, at a final concentration of 10 μM, LUF7244 did not significantly affect the APD in NRVMs as assesses by optical voltage mapping (**Figure IIIA**). In contrast, exposure of NRVM monolayers to 25 or 62.5 μM of LUF7244 decreased APD_{40} and significantly decreased APD_{90} to a similar extent. While the APD-shortening effect of LUF7244 was first observed at a final concentration of 25 μM, VU0405601 already caused a decrease of APD_{40} and a significant decrease APD_{90} at a final concentration of 10 μM (**Figure IIIB**). Raising the VU0405601 concentration to 25 or 62.5 μM did not lead to further APD shortening. Moreover, LUF7244 and VU0405601 had very similar maximum effects on the APD. Importantly, neither LUF7244 nor VU0405601 significantly changed the conduction velocity in the NRVM cultures at the 3 concentrations tested. These findings suggest that both LUF7244 and VU0405601 can increase I_{Kr} density but that VU0405601 is a more potent $K_v11.1$ activator than LUF7244.

Effects of LUF7244 on the Binding of [^{3}H]Astemizole to the hH_1R

To be of practical use in preventing drug-induced ventricular arrhythmias, LUF7244 should not interfere with the desired activities of unintended $K_v11.1$ blockers. We therefore tested whether LUF7244 affected binding of the antihistamine drug astemizole to the hH_1R. As displayed in **Figure VA**, LUF7244 did not decrease the binding of [^{3}H]astemizole to the hH_1R. Furthermore, the displacement curve of astemizole binding to the hH_1R was not significantly shifted rightwards by LUF7244 (**Figure VB**). Thus, LUF7244 reduces the affinity of the $K_v11.1$ channel for astemizole without affecting the binding of astemizole to its intended target receptor (*i.e.*, the hH_1R).

Effects of Prolonged Exposure of NRVMs to LUF7244 and/or Astemizole on Cell Viability, Excitability and Contractility

To study the effects of prolonged allosteric modulation and/or blockade of the $K_v11.1$ channel on the viability of cardiomyocytes, 6-day-old NRVM cultures were incubated for 72 hours in culture medium containing 10 μM LUF7244 and/or 100 nM astemizole. Subsequent staining with fluorescently labeled annexin V to detect cell surface-exposed phosphatidylserine yielded only very weak signals for cells exposed to vehicle, LUF7244, astemizole or LUF7244 plus astemizole, while NRVMs incubated for 24 hours with the proapoptotic drug doxorubicin displayed strong annexin V fluorescence (**Figure VIA**). These results indicate that prolonged exposure to 10 μM LUF7244 alone or in combination with 100 nM astemizole does not trigger programmed cell death.

Optical voltage mapping of 9-day-old NRVM cultures that had been mock-treated or treated for 72 hours with 10 μM LUF7244 and/or 100 nM astemizole produced very similar results as were obtained for cells that had only briefly been exposed to these compounds (compare **Figure 4** and **5** of the **Main Manuscript** with **Figure VIB** and **VIC**) and provided no indications for a drug-related reduction in excitability. Moreover, after electrical field stimulation cells in all four treatment groups displayed rhythmic contractions following the pacing frequency of 1 Hz (see **Supplemental Movies 1** through **4**).

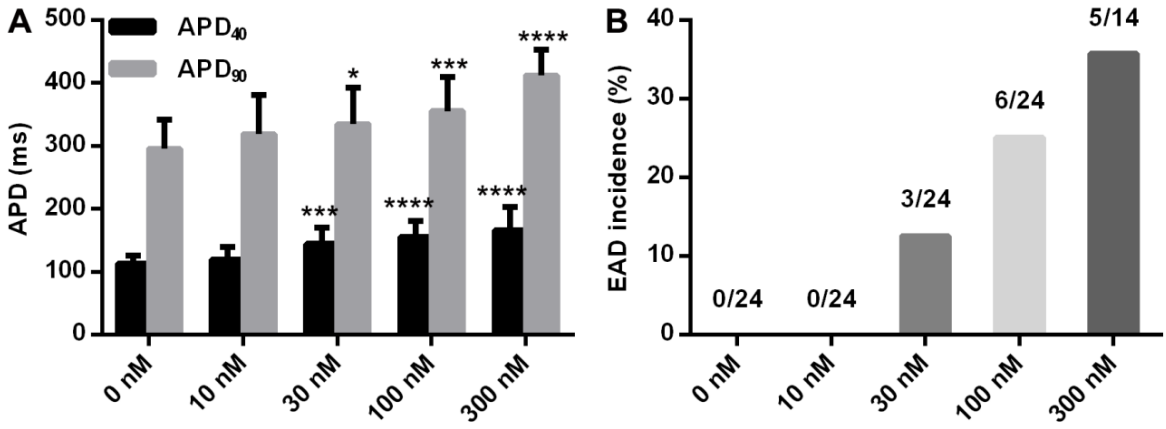

Figure I. Assessment, by optical voltage mapping, of the effect of different concentrations of astemizole on APD_{40} and APD_{90} (**A**) and EAD incidence (**B**) in NRVM monolayers. **P*<0.05, ****P*<0.001 and *****P*<0.0001.

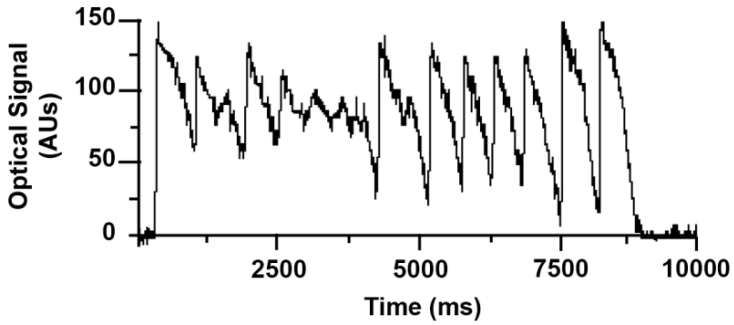

Figure II. Optical voltage trace showing an unstable, self-terminating tachyarrhythmia in an astemizole-treated NRVM culture following 1-Hz electrical point stimulation.

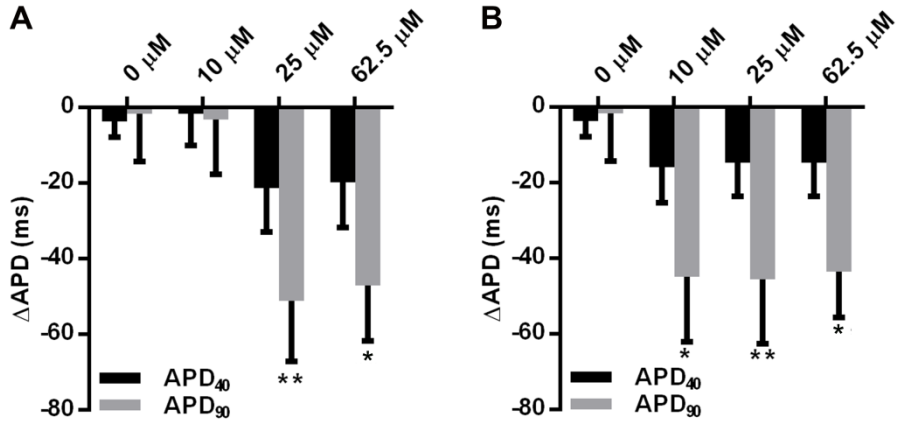

Figure III. Assessment, by optical voltage mapping, of the effect of different concentrations of LUF7244 (**A**) or VU0405601 (**B**) on APD_{40} and APD_{90}. Depicted are the pairwise average changes in APD (ΔAPD) caused by the treatment of NRVM cultures with vehicle or the indicated concentrations of LUF7244 or VU0405601 for 30 min. **P*<0.05 and ***P*<0.01 vs vehicle-treated NRVM cultures. No significant differences in APD_{40} and APD_{90} were observed between the cell cultures exposed to 25 and 62.5 μM LUF7244 and between the NRVM monolayers treated with 10, 25 or 62.5 μM VU0405601. (n=6 per group)

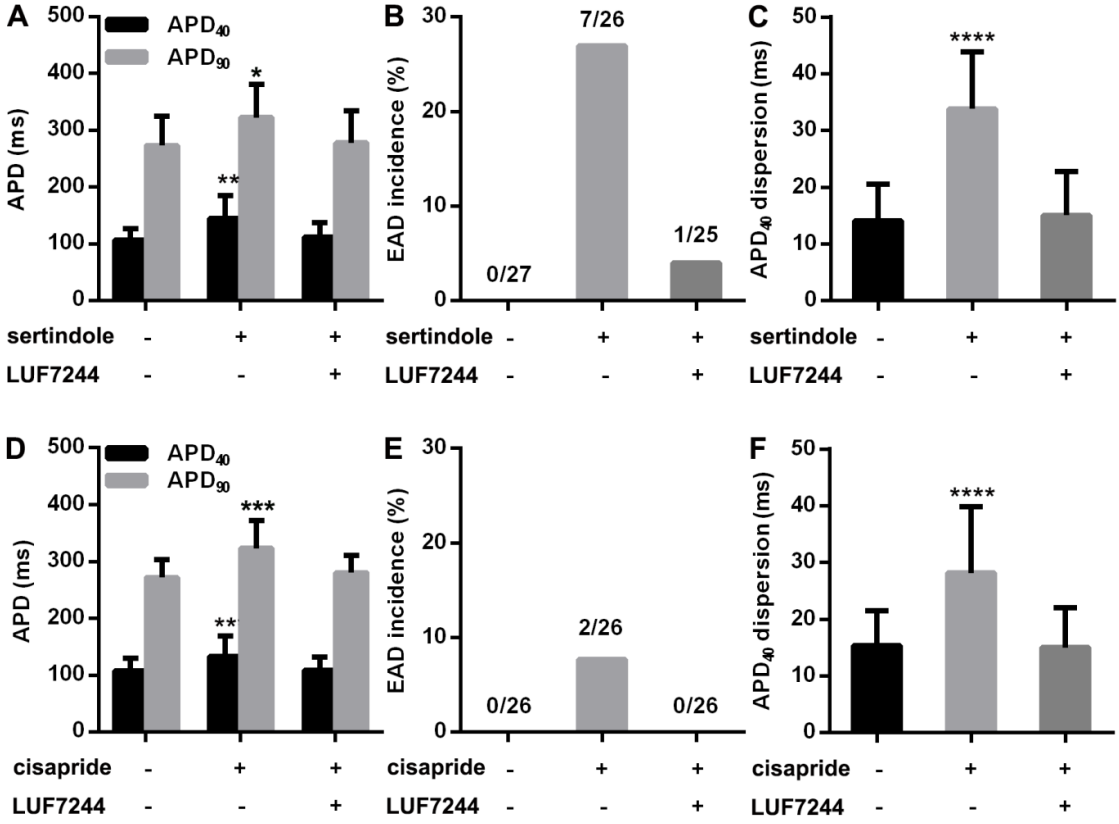

Figure IV. Assessment, by optical voltage mapping, of the ability of LUF7244 to counteract the proarrhythmic effects of sertindole and cisapride on NRVMs. Pretreatment of NRVM cultures with LUF7244 completely prevented the increase in APD_{40} and APD_{90} (**A** and **D**), EAD incidence (**B** and **E**) and APD_{40} dispersion (**C** and **F**) induced by exposure of the cells to 1 μM sertindole (**A**, **B** and **C**) or 1 μM cisapride (**D**, **E** and **F**). **P*<0.05, ***P*<0.01, ****P*<0.001 and *****P*<0.0001.

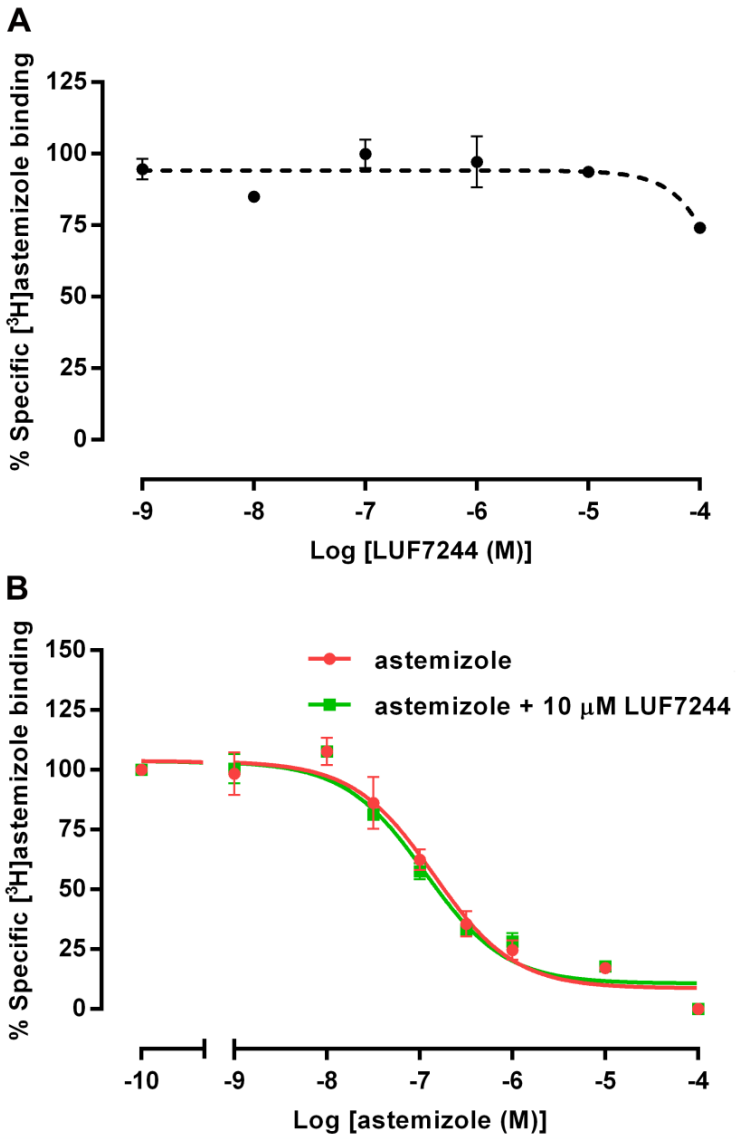

Figure V. Assessment of the effects of LUF7244 on the binding of astemizole to the hH_1R in a [^{3}H]astemizole binding assay performed with membranes of HEK293hH_1R cells. **A:** Displacement curve of LUF7244. **B:** Displacement curve of astemizole in the absence or presence of 10 µM LUF7244.

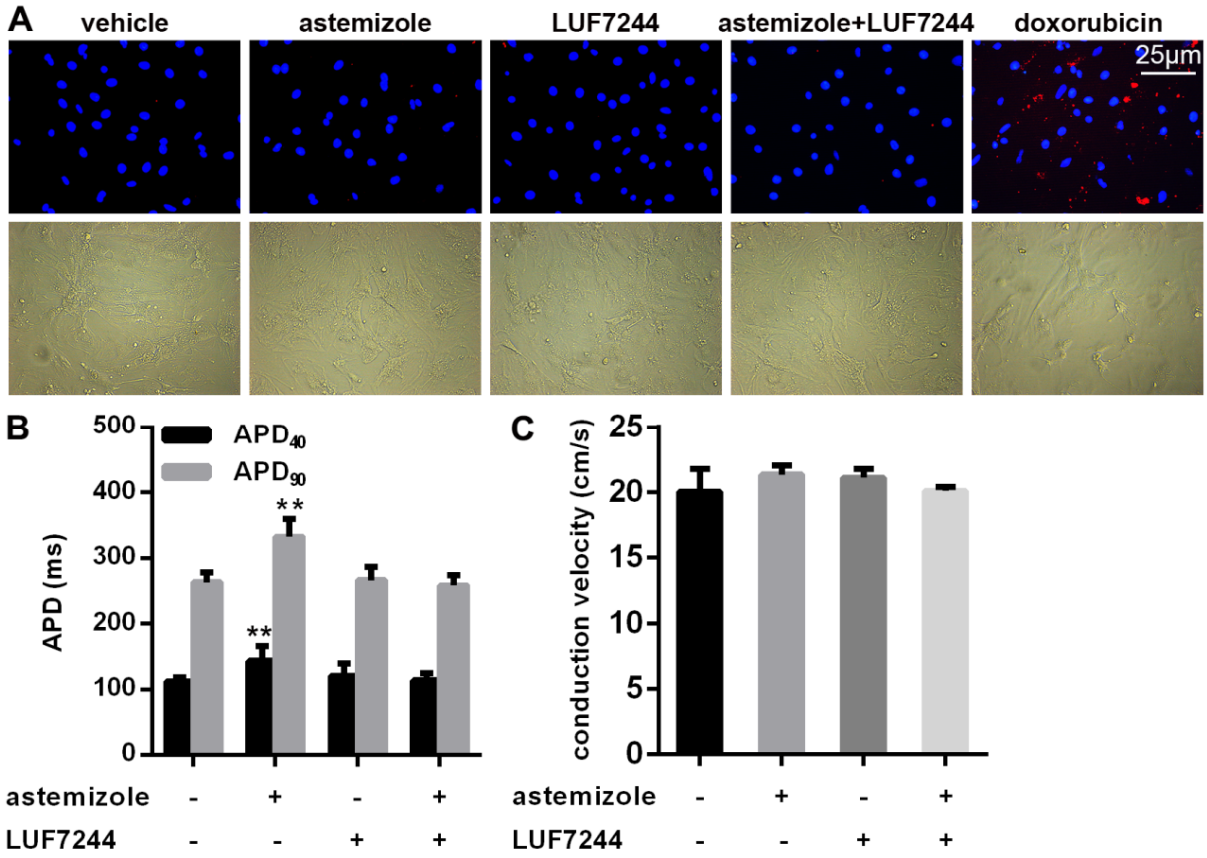

Figure VI. Effects of prolonged exposure of NRVMs to LUF7244 and/or astemizole on cell viability and excitability. **A:** Analysis by Alexa Fluor-568-conjugated annexin V staining of cell surface expression of phosphatidylserine as early marker of apoptosis. NRVM cultures exposed for 72 hours to vehicle, 10 µM LUF7244, 100 nM astemizole or 10 µM LUF7244 plus 100 nM astemizole showed very weak signals, while NRVMs incubated for 24 hours with 1 µM of the proapoptotic drug doxorubicin displayed strong annexin V-associated red fluorescence. The blue fluorescence corresponds to cell nuclei stained with the DNA-binding due Hoechst 33342. **B:** Quantitative comparison of APD_{40} and APD_{90} in NRVM cultures exposed for 72 hours to vehicle, 10 µM LUF7244, 100 nM astemizole or 10 µM LUF7244 plus 100 nM astemizole. $^{**}P<0.01$. **C:** Quantitative comparison of CV in NRVM cultures exposed for 72 hours to vehicle, 10 µM LUF7244, 100 nM astemizole or 10 µM LUF7244 plus 100 nM astemizole. (n=6 per group)

Table I. The half maximal inhibitory concentrations (IC_{50}), percentage specific binding of [^{3}H]dofetilide to the K_v11.1 channel after 6 minutes of dissociation in the absence (control) or presence of 10 μM indicated compounds (%$B/B_{control}$), and dissociation rate (k_{off}) of [^{3}H]dofetilide in the absence (control) or presence of 50 μM indicated compounds.

	IC_{50} (nM)	%$B/B_{control}$	k_{off} (min^{-1})
dofetilide	-	100±0.01	0.21±0.02
+VU0405601	7,757±350	63±3**	0.42±0.04**
+ML-T531	12,000±1,213	77±3**	0.30±0.03*
+LUF7244	3,855±724	44±2**	0.33±0.02**

All values for comparison are means (±SEM) of six samples except that k_{off} values of dofetilide in the absence of indicated compounds or presence of 50 μM ML-T531 are derived from seven samples. Statistical analysis of the results is conducted by Mann-Whitney U test (*P<0.05 vs control; **P<0.01 vs control).

Table II. The K_v11.1 affinities (K_i) of dofetilide, astemizole, sertindole and cisapride in the absence (control) or presence of 10 μM LUF7244.

	K_i (nM)	K_i + 10 μM LUF7244 (nM)	Fold Change
dofetilide	6.2±0.3	20±5*	3.2
astemizole	0.97±0.04	3.7±0.2**	3.8
sertindole	21±2	47±7**	2.2
cisapride	21±1	85±6**	4.0

All values for comparison are means (±SEM) of six samples. Statistical analysis of the results is conducted by Mann-Whitney U test (*P<0.05 vs control; **P<0.01 vs control).

Supplemental Discussion

Clinical Applicability of Allosteric K_v11.1 Modulators

A major concern and obstacle for medicinal chemists involved in the development of drugs to remedy congenital and acquired long QT syndrome is excessive APD shortening resulting in short QT syndrome (SQTS).[9,10] For instance, at a concentration of 10 μM, the potent K_v11.1 activator ICA-105574 shortened the APD in Langendorff-perfused guinea pig hearts by 34% and induced non-"*Torsades de Pointes*"-like ventricular arrhythmias in 2 out of 8 animals.[11] Likewise, in a transgenic rabbit model of LQT1, shortening of the QTc interval by another K_v11.1 activator designated NS1643 was accompanied by an increased incidence of pacing-induced ventricular fibrillation.[12] However, the fact that LUF7244 at a concentration that completely abolished the proarrhythmic effects of astemizole, sertindole and cisapride does not shorten the APD of NRVMs and therefore may not give rise to drug-induced SQTS raises hope for its clinical applicability.

For the experiments in NRVM monolayers, the final astemizole concentration was 100 nM in most cases, while sertindole and cisapride were used at a final concentration of 1 μM. These concentrations are much higher than the therapeutic blood concentrations of these fortuitous K_v11.1 blockers, which are 2-50 μg/L (*i.e.*, 4.4-109 nM) for astimizole, 40-80 μg/L (*i.e.*, 86-172 nM) for cisapride and 50-100 μg/L (*i.e.*, 113-227 nM) for sertindole.[13] The proarrhythmic effects of these drugs on NRVMs were completely prevented by 10 μM (*i.e.*, 3.7 mg/L) LUF7244, a concentration that did not negatively influence the binding of astemizole to the hH_1R and did not noticeably affect the viability, contractility and excitability of the cardiomyocytes (see "*Effects of Prolonged Exposure of NRVMs to LUF7244 and/or Astemizole on Cell Viability, Excitability and Contractility*"). Accordingly, blood LUF7244 concentrations well below 10 μM may suffice to counteract the proarrhythmic effects of unintended K_v11.1 blockers in humans. However, before LUF7244 or other K_V11.1 allosteric modulators can be clinically applied as "*co-drugs*" or otherwise, they should be subjected to rigorous preclinical and clinical testing with appropriate pharmacokinetic and pharmacodynamics assessments to determine their benefit-risk profiles.

Supplemental References

1. Shagufta, Guo D, Klaasse E, de Vries H, Brussee J, Nalos L, Rook MB, Vos MA, van der Heyden MA, IJzerman AP. Exploring chemical substructures essential for hERG K^+ channel blockade by synthesis and biological evaluation of dofetilide analogues. *ChemMedChem.* 2009;4:1722-1732.
2. Ficker E, Dennis AT, Wang L, Brown AM. Role of the cytosolic chaperones hsp70 and hsp90 in maturation of the cardiac potassium channel hERG. *Circ Res.* 2003;92:e87-e100.
3. Yu Z, Klaasse E, Heitman LH, IJzerman AP. Allosteric modulators of the hERG K^+ channel: Radioligand binding assays reveal allosteric characteristics of dofetilide analogs. *Toxicol Appl Pharmacol.* 2014;274:78-86.
4. Pijnappels DA, Schalij MJ, Ramkisoensing AA, van Tuyn J, de Vries AA, van der Laarse A, Ypey DL, Atsma DE. Forced alignment of mesenchymal stem cells undergoing cardiomyogenic differentiation affects functional integration with cardiomyocyte cultures. *Circ Res.* 2008;103:167-176.
5. Askar SF, Ramkisoensing AA, Schalij MJ, Bingen BO, Swildens J, van der Laarse A, Atsma DE, de Vries AA, Ypey DL, Pijnappels DA. Antiproliferative treatment of myofibroblasts prevents arrhythmias in vitro by limiting myofibroblast-induced depolarization. *Cardiovasc Res.* 2011;90:295-304.
6. Cheng Y, Prusoff WH. Relationship between the inhibition constant (K_i) and the concentration of inhibitor which causes 50 percent inhibition (I_{50}) of an enzymatic reaction. *Biochem Pharmacol.* 1973;22:3099-3108.
7. Yu Z, IJzerman A, Heitman L. K_v11.1 (hERG)-induced cardiotoxicity: A molecular insight from a binding kinetics study of prototypic K_v11.1 (hERG) inhibitors. *Br J Pharmacol.* 2015;172:940-945.
8. Potet F, Lorinc AN, Chaigne S, Hopkins CR, Venkataraman R, Stepanovic SZ, Lewis LM, Days E, Sidorov VY, Engers DW, Zou B, Afshartous D, George AL Jr, Campbell CM, Balser JR, Li M, Baudenbacher FJ, Lindsley CW, Weaver CD, Kupershmidt S. Identification and characterization of a compound that protects cardiac tissue from human ether-a-go-go-related gene (hERG)-related drug-induced arrhythmias. *J Biol Chem.* 2012;287:39613-39625.
9. Sanguinetti MC. hERG1 channel agonists and cardiac arrhythmia. *Curr Opin Pharmacol.* 2014;15:22-27.
10. Grunnet M, Hansen RS, Olesen S-P. hERG1 channel activators: A new anti-arrhythmic principle. *Prog Biophys Mol Biol.* 2008;98:347-362.
11. Meng J, Shi C, Li L, Du Y, Xu Y. Compound ICA-105574 prevents arrhythmias induced by cardiac delayed repolarization. *Eur J Pharmacol.* 2013;718:87-97.
12. Bentzen BH, Bahrke S, Wu K, Larsen AP, Odening KE, Franke G, Biermann J, Peng X, Koren G, Zehender M. Pharmacological activation of K_v11.1 in transgenic long QT-1 rabbits. *J Cardiovasc Pharmacol.* 2011;57:223-230.
13. Schulz M, Iwersen-Bergmann S, Andresen H, Schmoldt A. Therapeutic and toxic blood concentrations of nearly 1,000 drugs and other xenobiotics. *Critical Care.* 2012;16:R136.